NASA TN D-1149

TECHNICAL NOTE

D-1149

LONGITUDINAL FORCE AND MOMENT DATA AT MACH NUMBERS FROM 0.60 TO 1.40 FOR A FAMILY OF ELLIPTIC CONES WITH VARIOUS SEMIAPEX ANGLES

By Louis S. Stivers, Jr., and Lionel L. Levy, Jr.

Ames Research Center
Moffett Field, Calif.

NATIONAL AERONAUTICS AND SPACE ADMINISTRATION

WASHINGTON

December 1961

NATIONAL AERONAUTICS AND SPACE ADMINISTRATION

TECHNICAL NOTE D-1149

LONGITUDINAL FORCE AND MOMENT DATA AT MACH NUMBERS FROM 0.60 TO 1.40 FOR A FAMILY OF ELLIPTIC CONES WITH VARIOUS SEMIAPEX ANGLES

By Louis S. Stivers, Jr., and Lionel L. Levy, Jr.

SUMMARY

An investigation has been made to determine the aerodynamic characteristics of four elliptic cones having plan-form semiapex angles ranging from about 9° to 31°, and also for one of these cones modified on the upper surface to reduce the base area by about one half. The tests were made for angles of attack from about -2° to +21°, at Mach numbers from 0.60 to 1.40, and for a constant Reynolds number of 1.4 million, based on the length of the models.

For each model, lift, pitching-moment, and drag coefficients, and lift-drag ratios are presented for the forebody, and axial-force coefficients are presented for the base. Calculated lift and pitching-moment curves for the elliptic cones, and lift-curve slopes for each model at supersonic Mach numbers are shown for comparison with the corresponding experimental values. Lift-drag ratios are also given for the forebody and base combined. These data are presented without discussion.

INTRODUCTION

The elliptic-cone shape is basic to some lifting configurations presently contemplated for re-entry vehicles. Experimental aerodynamic characteristics of elliptic cones are available for low speeds and for supersonic speeds. (See refs. 1 to 8.) It is the purpose of this report to supplement the available experimental data with the results of additional tests made at Mach numbers from 0.6 to 1.4. Data are presented for four elliptic-cone models with plan-form semiapex angles ranging from about 9° to 31°, and also for one of these models modified on the upper surface to reduce the base area by about one half. Tests of the five models were made for angles of attack from about -2° to +21°.

NOTATION

B	area of model base
$\bar{c}$	mean aerodynamic chord of model plan form, two-thirds of model length
C_{A_b}	base axial-force coefficient (positive rearward), $\frac{\text{base axial force}}{qB}$
C_D	drag coefficient of forebody (excluding base drag coefficient), $\frac{\text{forebody drag}}{qS}$
C_L	lift coefficient of forebody
$C_{L_{total}}$	lift coefficient of forebody and base combined
C_{L_α}	lift-curve slope of forebody at low incidence, $\frac{dC_L}{d\alpha}$, per radian
C_m	pitching-moment coefficient of forebody referred to $\frac{\bar{c}}{2}$ (see fig. 1), $\frac{\text{forebody pitching moment about axis through } \bar{c}/2}{qS\bar{c}}$
d	distance of model base centroid of area above chord plane which contains moment center and major axis of elliptic profile
$\frac{d}{\bar{c}}$	dimensionless centroidal distance
K	cross-flow constant
l	length of model, in.
$\frac{L}{D}$	lift-drag ratio of forebody, $\frac{C_L}{C_D}$
$(\frac{L}{D})_{total}$	lift-drag ratio of forebody and base combined
M	Mach number
q	free-stream dynamic pressure
R	Reynolds number

$\frac{R}{l}$ unit Reynolds number, millions per inch

S plan-form area of model

α angle of attack of model

ϵ plan-form semiapex angle of model

APPARATUS AND TESTS

Wind Tunnel

The tests were conducted in the Ames 2- by 2-Foot Transonic Wind Tunnel. This tunnel utilizes a flexible nozzle and porous test-section walls to permit continuous operation up to a Mach number of 1.4, and to provide choke-free flow in the test section throughout the transonic Mach number range. A constant Reynolds number is maintained throughout the operational range of Mach numbers by controlling the stagnation pressure within the tunnel.

Models and Equipment

The five models employed in the present tests are illustrated in figure 1. Four of the models are elliptic cones (models A through D) with plan-form semiapex angles of 8.57°, 15.00°, 22.73°, and 31.08°, and each has a ratio of cross-section thickness to width of 1/3 and a base area of 4.712 square inches. The fifth model (E) is the elliptic cone with a plan-form semiapex angle of 15.00° with the upper surface modified, as illustrated in figures 1(b) and (c), to reduce the base area. For this model the base area is 2.367 square inches.

Boundary-layer transition wires were attached with lacquer to the surface of each model. The diameter of the wires used, varying from 0.009 inch for model A to 0.004 inch for model D, was selected so as to maintain a nearly constant Reynolds number of the wire during the tests. (The tests were made for various values of unit Reynolds number, R/l, to provide a constant Reynolds number of 1.4 million based on the length of the models.) A wire was placed around each model near the apex at a longitudinal station 7 percent of the root chord measured from the apex. Between this station and the model base, along rays located at a distance of 45 percent of the local span on each side of the plane of symmetry of the models, additional wires were positioned on the upper and lower surfaces of the elliptic-cone models, A through D, and on the lower surface of the modified model, E. (See fig. 1.)

The models were mounted on a flexure-type strain-gage balance supported by a 0.688-inch-diameter sting. Only for model A was this balance enclosed within the model. For all the other models the exposed portion of the balance was shielded from the airstream by a 0.875-inch-diameter shroud which covered the balance and the sting. The ratio of sting length (distance from model base to sting flare) to sting or shroud diameter differed for each model, varying from 6.8 for model A to 10.7 for model D. The sting-flare half-angle was 4.7°.

Tubes for measuring static pressures were located at the base of the models; 4 tubes were used with the elliptic cones, and 16 tubes with the modified elliptic cone.

Tests

Lift, pitching-moment, drag, and base-pressure data were obtained for each model at 13 Mach numbers ranging from 0.60 to 1.40, and for angles of attack from about -2° to +21°. In addition, corresponding data were obtained at a Mach number of 0.60 for the modified cone inverted. The Reynolds number was held constant at a value of 1.4 million, based on the length of the models. All measurements were made with the transition wires in place on each model. The visualization technique described in reference 9 was used to establish the effectiveness of the wires in producing a turbulent boundary layer.

CORRECTIONS AND PRECISION

The base-pressure measurements for the elliptic cones have been corrected for the effects of the sting supports by means of the data of reference 10. Although the data of this reference are applicable strictly to model B, the corrections were assumed to apply also to the other elliptic-cone models. The magnitude of the corrections relative to the total drag of the forebody and base combined varied with each model from 31 percent for model A to 15 percent for model D. Corrections have not been applied to the base-pressure data for model E, the modified elliptic cone, since no appropriate sting-support corrections were known. The corrections, however, would affect a smaller base area on model E than on the elliptic cone models, and the base drag would be a smaller part of the total drag.

No wall-interference corrections have been applied to the data of this report. Such corrections are believed to be small for the present tests except, possibly, for Mach numbers near unity. Other factors that

could have influenced the measured data have been evaluated and found to be insignificant. These factors have been neglected.

In addition to any systematic errors that might be introduced by the combination of corrections that have been neglected, the test data are also subject to random errors of measurement which would affect the reliability of the data. The standard deviations or mean square errors in Mach number, angle of attack, and Reynolds number, and lift, pitching-moment, drag, and base axial-force coefficients for the present tests have been evaluated by the method of reference 11. Representative values are given in the following table:

Standard deviations						
Item	M=0.60		M=1.00		M=1.40	
	α=2°	α=12°	α=2°	α=12°	α=2°	α=12°
M	±0.002	±0.002	±0.002	±0.002	±0.003	±0.003
α	±0.03°	±0.03°	±0.03°	±0.03°	±0.03°	±0.03°
R	$\pm 0.003 \times 10^6$	$\pm 0.003 \times 10^6$	$\pm 0.005 \times 10^6$	$\pm 0.005 \times 10^6$	$\pm 0.005 \times 10^6$	$\pm 0.005 \times 10^6$
C_L	±0.002	±0.005	±0.001	±0.006	±0.001	±0.006
C_m	±0.001	±0.003	±0.001	±0.003	±0.001	±0.003
C_D	±0.002	±0.002	±0.004	±0.004	±0.003	±0.004
C_{A_b}	±0.006	±0.006	±0.005	±0.005	±0.004	±0.004

RESULTS

The results are presented as follows without discussion. Lift, pitching-moment, and drag coefficients for the forebody of each model are shown in figures 2 to 7 as functions of angle of attack and Mach number. Forebody lift-drag ratios are presented in figure 8. Axial-force coefficients for the base of each model are shown in figures 9 and 10 as functions of angle of attack and Mach number, respectively.

Total coefficients associated with the combination of the forebody and base of each model may be determined by the following relations:

$$C_{L_{total}} = C_L - \frac{B}{S} C_{A_b} \sin \alpha$$

$$C_{m_{total}} = C_m + \frac{B}{S} C_{A_b} \frac{d}{\bar{c}}$$

$$C_{D_{total}} = C_D + \frac{B}{S} C_{A_b} \cos \alpha$$

The value of $d/\bar{c}$ is zero for the elliptic cones, and -0.0255 and +0.0255 for the modified cone upright and inverted, respectively. Inasmuch as the total aerodynamic characteristics of the combined forebody and base are substantially different from the characteristics of the forebody alone, because of the large drag contribution of the base, total lift-drag ratios have also been determined for each model and are presented in figure 11.

An attempt was made to predict the variations of lift with angle of attack for the four elliptic cones by adding a cross-flow lift to that determined by linear theory. The lift was computed using the relation (see refs. 12 and 13)

$$C_L = \alpha\left(\frac{dC_L}{d\alpha}\right)_{\substack{\text{linear} \\ \text{theory}}} + K\alpha^2$$

For the computations, the linear-theory lift-curve slopes for subsonic and supersonic Mach numbers were determined by the methods of references 14 and 15, respectively. The value of K was assumed to be 1.2. A comparison of the calculated and experimental lift curves for the elliptic cones is shown in figure 12. The experimental lift-curve slopes for each model at the supersonic Mach numbers are presented in figure 13, as a function of $\sqrt{M^2-1}$ tangent ϵ, together with the corresponding slopes given by the linear theory of reference 15.

Calculated curves of the variation of pitching-moment coefficient with lift coefficient were also determined for the elliptic cones using the linear theories of references 16 and 15 for subsonic and supersonic Mach numbers, respectively. Since the cross flow is generally considered to act through the centroid of plan-form area of a body, a cross-flow term would not enter the present pitching-moment calculations. A comparison of the calculated and experimental pitching-moment curves is shown in figure 14.

Ames Research Center
National Aeronautics and Space Administration
Moffett Field, Calif., Oct. 4, 1961

REFERENCES

1. Fink, P. T.: Some Low Speed Aerodynamic Properties of Cones. Experiments Done in the Imperial College Aeronautical Laboratory. British ARC 17,632, Perf. 1363, S & C 3014, F.M. 2250, 1955.

2. McDevitt, John B., and Rakich, John V.: The Aerodynamic Characteristics of Several Thick Delta Wings at Mach Numbers to 6 and Angles of Attack to 50°. NASA TM X-162, 1960.

3. Rogers, E. W. E., and Berry, C. J.: Experiments at M=1.41 on Elliptic Cones with Subsonic Leading Edges. British ARC 17,929, F.M. 2307, Perf. 1391, 1955. (Also ARC R&M 3042, 1958)

4. Jorgensen, Leland H.: Elliptic Cones Alone and With Wings at Supersonic Speeds. NACA Rep. 1376, 1958. (Supersedes NACA TN 4045)

5. Wiggins, Lyle E., and Kaattari, George E.: Supersonic Aerodynamic Characteristics of Triangular Plan-Form Models at Angles of Attack to 90°. NASA TM X-568, 1961.

6. Jackson, Charlie M., Jr., and Harris, Roy V., Jr.: Investigation at a Mach Number of 1.99 of Two Series of Blunted Delta Planform Models With Several Cross-Sectional Shapes for Angles of Attack From 0° to 90°. NASA TM X-543, 1961.

7. Zakkay, Victor, and Visich, Marion, Jr.: Experimental Pressure Distributions on Conical Elliptical Bodies at $M_\infty = 3.09$ and 6.0. Polytechnic Institute of Brooklyn Rep. 467, 1959. (Also OSR TN 59-10.)

8. Chapkis, Robert L.: Hypersonic Flow Over an Elliptic Cone: Theory and Experiment. Guggenheim Aeronautical Laboratory, Calif. Inst. of Tech., Hypersonic Research Project Memo. 49, 1959.

9. Main-Smith, J. D.: Chemical Solids as Diffusible Coating Films for Visual Indications of Boundary-Layer Transition in Air and Water. British A.R.C. R&M 2755 (13,115), 1954. (Also R.A.E. Chem. 466, Feb. 1950.)

10. Stivers, Louis S., Jr., and Levy, Lionel L., Jr.: Effects of Sting-Support Diameter on the Base Pressures of an Elliptic Cone at Mach Numbers From 0.60 to 1.40. NASA TN D-354, 1961.

11. Beers, Yardley: Introduction to the Theory of Error. Addison-Wesley Publishing Co., Cambridge, Mass., 1953.

12. Allen, H. Julian, and Perkins, Edward W.: A Study of Effects of Viscosity on Flow Over Slender Inclined Bodies of Revolution. NACA Rep. 1048, 1951. (Supersedes NACA TN 2044)

13. Flax, A. H., and Lawrence, H. R.: The Aerodynamics of Low-Aspect-Ratio Wings and Wing-Body Combinations. Third Anglo-American Aeronautical Conference, Brighton, 4th-7th September 1951. Convened by the R.A.S. and I.A.S., Joan Bradbrooke and E. G. Pike, eds., 1952, pp. 363-398. (Published also as Rep. CAL-37, Cornell Aeronautical Lab., Inc., Buffalo, 1951).

14. DeYoung, John, and Harper, Charles W.: Theoretical Symmetric Span Loading at Subsonic Speeds for Wings Having Arbitrary Plan Form. NACA Rep. 921, 1948.

15. Puckett, A. E., and Stewart, H. J.: Aerodynamic Performance of Delta Wings at Supersonic Speeds. Jour. Aero. Sci., vol. 14, no. 10, Oct. 1947, pp. 567-578.

16. Lomax, Harvard, and Sluder, Loma: Chordwise and Compressibility Corrections to Slender-Wing Theory. NACA Rep. 1105, 1952. (Supersedes NACA TN 2295)

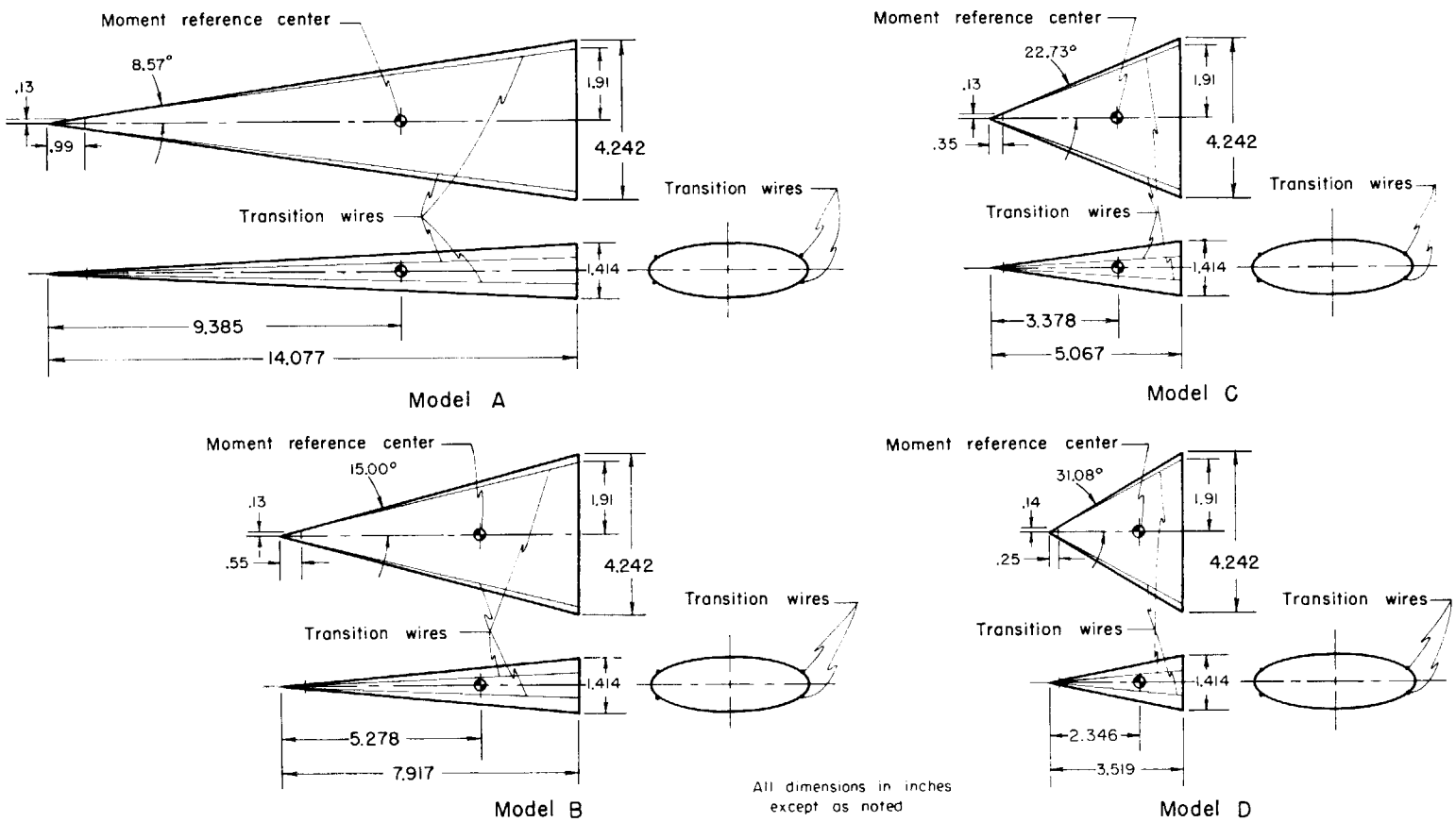

(a) The elliptic-cone models.

Figure 1.- Geometrical information for the models.

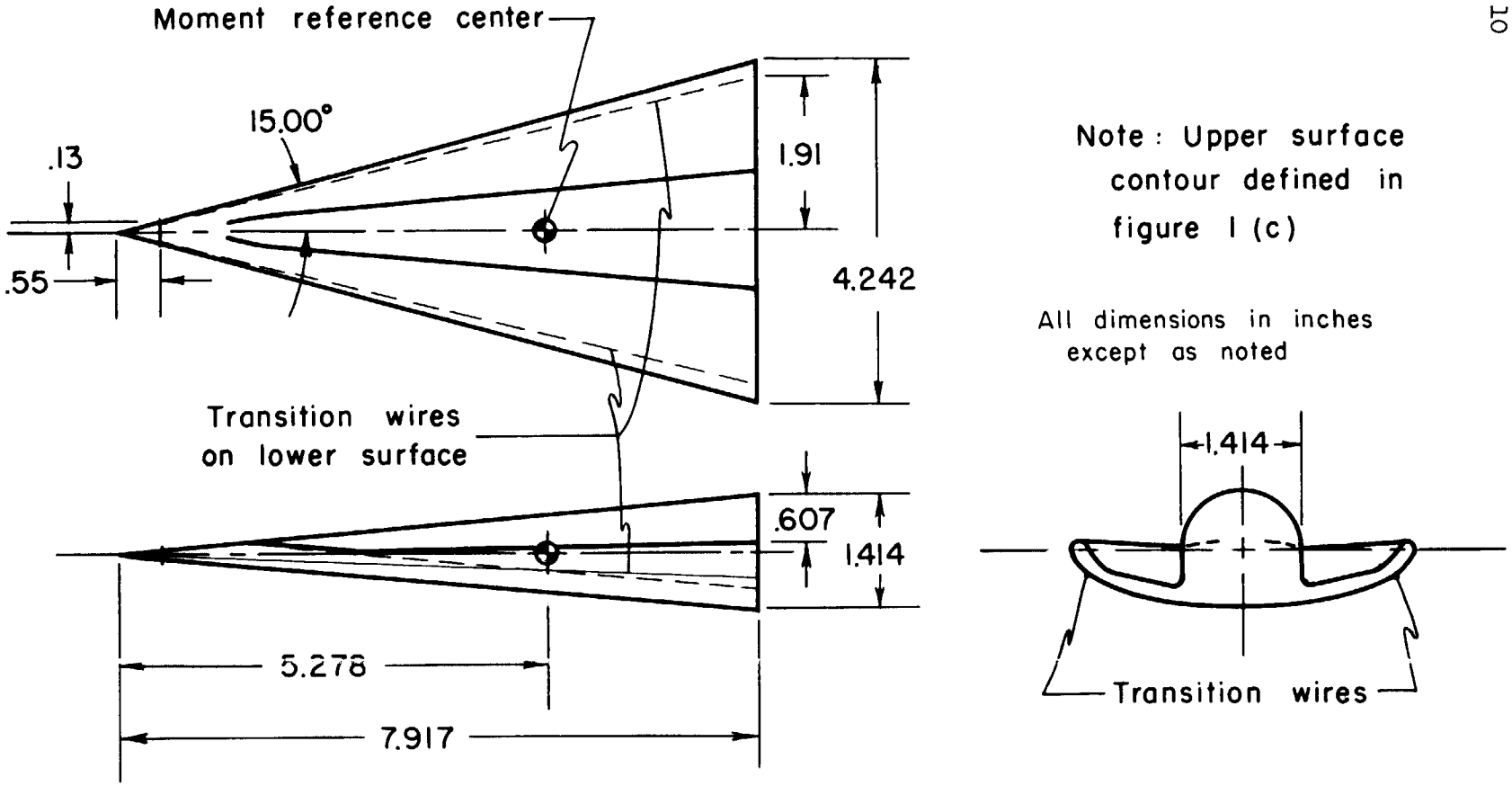

Model E

(b) The modified elliptic-cone model.

Figure 1.- Continued.

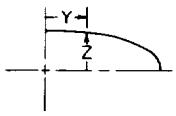

Sta. 1.167

Y	0	.037	.074	.110	.147	.165	.184	.202	.220	.239	.257	.276	.294	.307	.311	.312
Z	.104	.103	.101	.097	.092	.088	.084	.079	.074	.067	.059	.049	.035	.017	.009	0

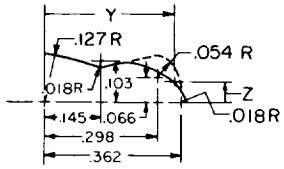

Sta. 1.417

Y	.201	.224	.246	.268	.291	.313	.336
Z	.107	.102	.096	.090	.081	.071	.059

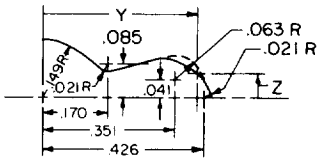

Sta. 1.667

Y	.316	.343	.369	.396	.422
Z	.106	.096	.084	.070	.050

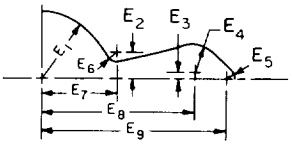

Sta.	E_1	E_2	E_3	E_4	E_5	E_6	E_7	E_8	E_9
1.917	.171 R	.066	.016	.073R	.024 R	.024 R	.195	.403	.489
2.167	.194 R	.048	.009	.082R	.027 R	.027R	.221	.456	.554
2.417	.216 R	.030	.034	.092R	.030R	.030R	.246	.508	.616

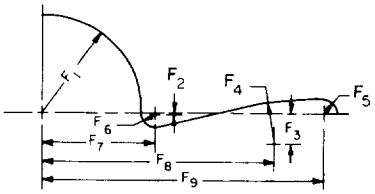

Sta.	F_1	F_2	F_3	F_4	F_5	F_6	F_7	F_8	F_9
2.917	.260 R	.007	.084	.110 R	.037 R	.037 R	.297	.612	.744
3.258	.291 R	.034	∞	∞	.041 R	.041 R	.332	–	.831

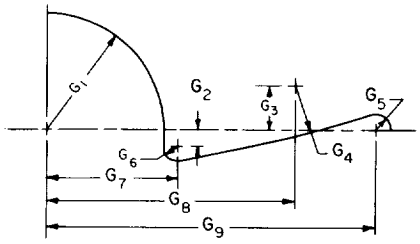

Sta.	G_1	G_2	G_3	G_4	G_5	G_6	G_7	G_8	G_9
3.417	.305 R	.044	.118	.130 R	.043 R	.043 R	.348	.660	.873
3.917	.350 R	.080	.105	.148 R	.050 R	.050R	.400	.756	1.000
7.917	.707 R	.374	0	.300R	.100 R	.100R	.807	1.528	2.021

All dimensions in inches

(c) Upper surface contours of the modified elliptic cone for various longitudinal stations measured from the cone apex.

Figure 1.- Concluded.

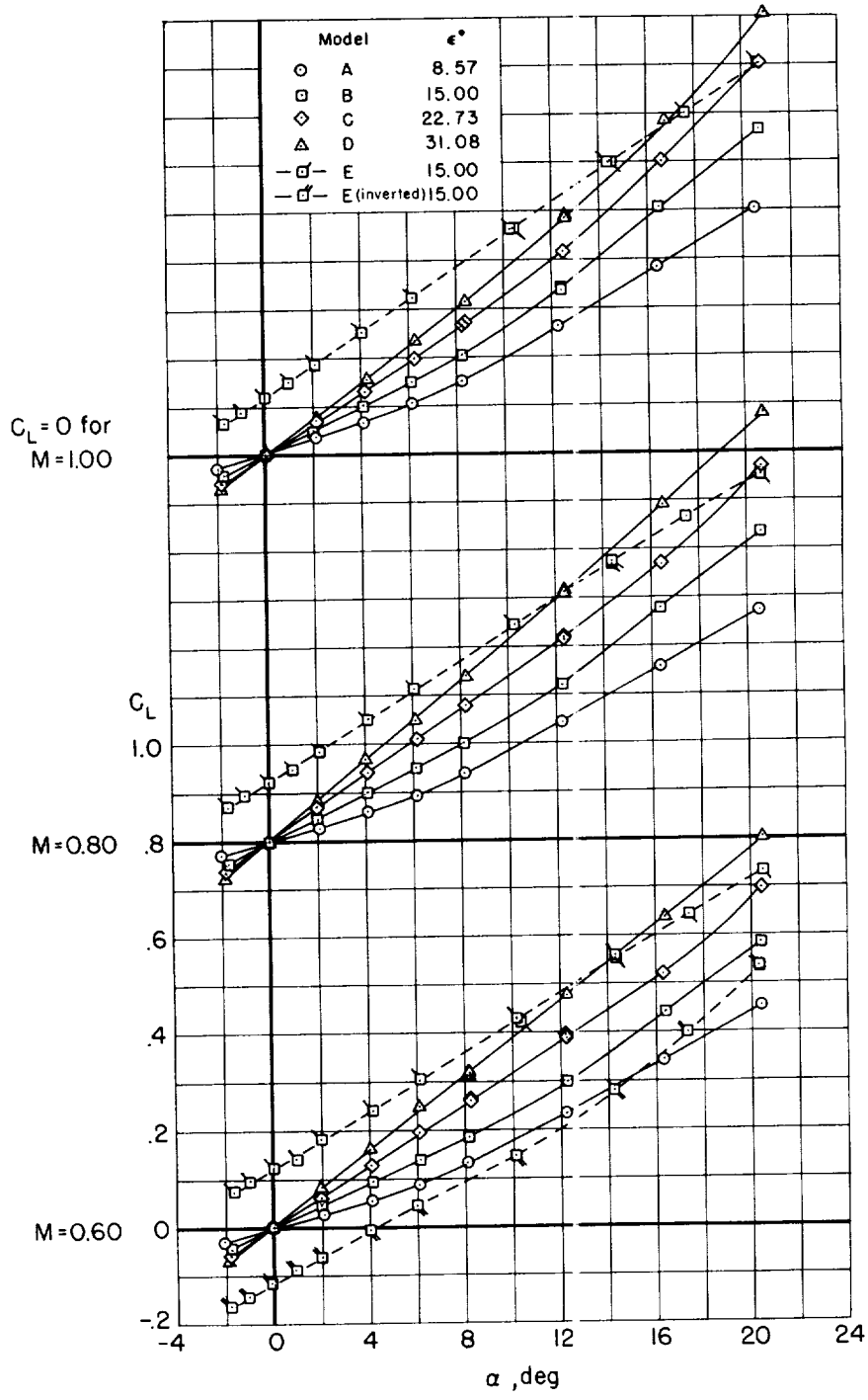

(a) M = 0.60, 0.80, and 1.00

Figure 2.- Variation of forebody lift coefficient with angle of attack.

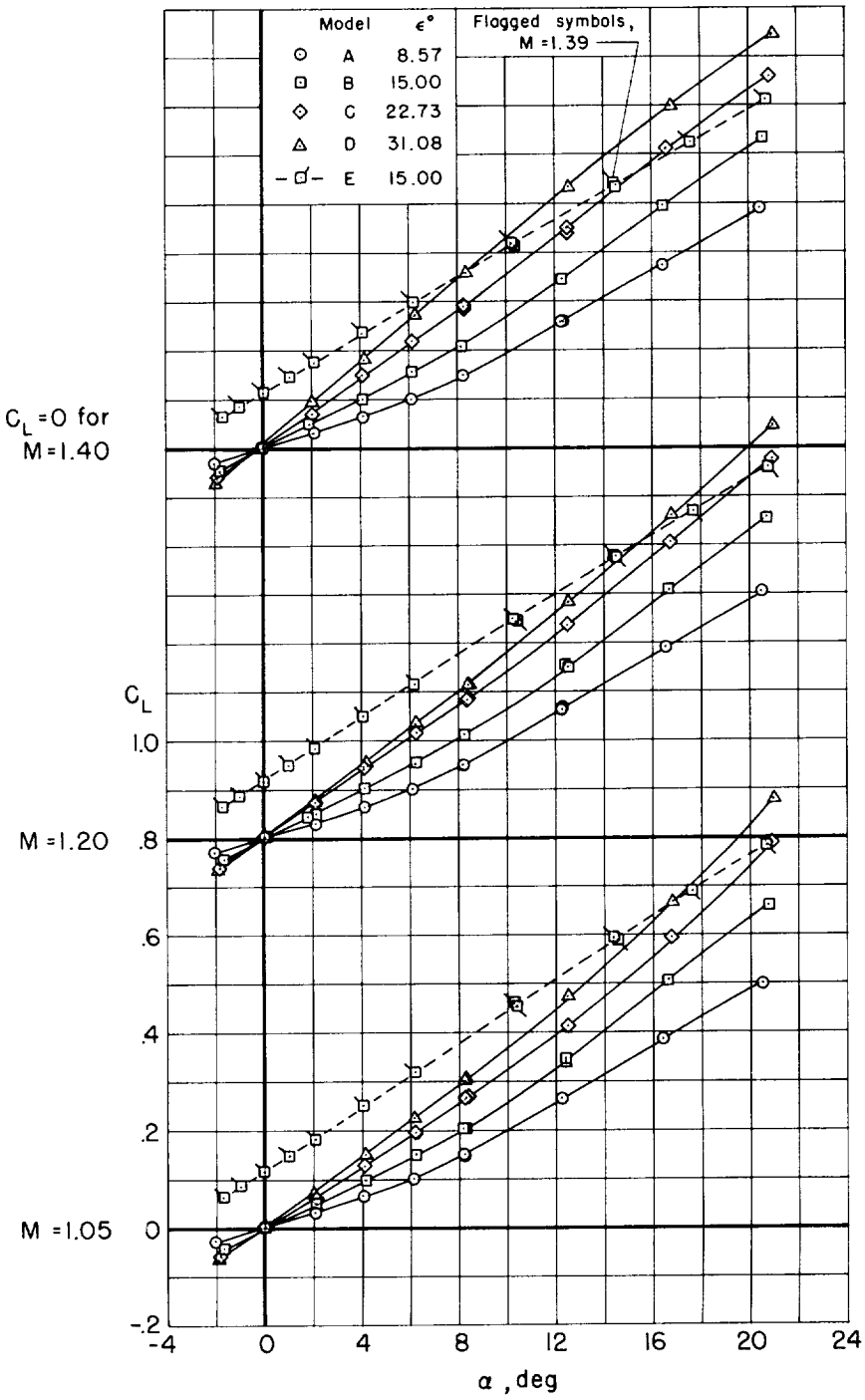

(b) M = 1.05, 1.20, and 1.40

Figure 2.- Concluded.

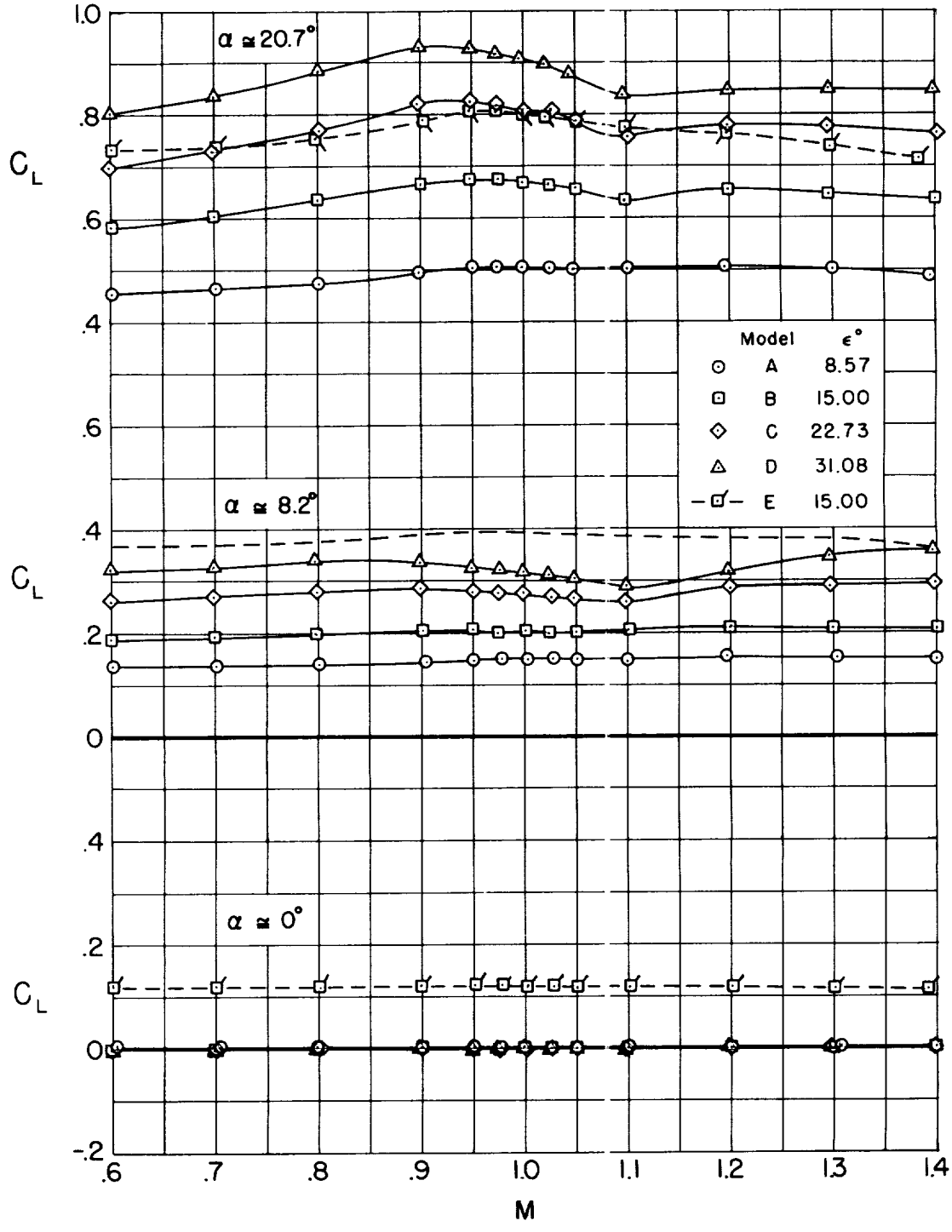

Figure 3.- Effect of Mach number on forebody lift coefficient.

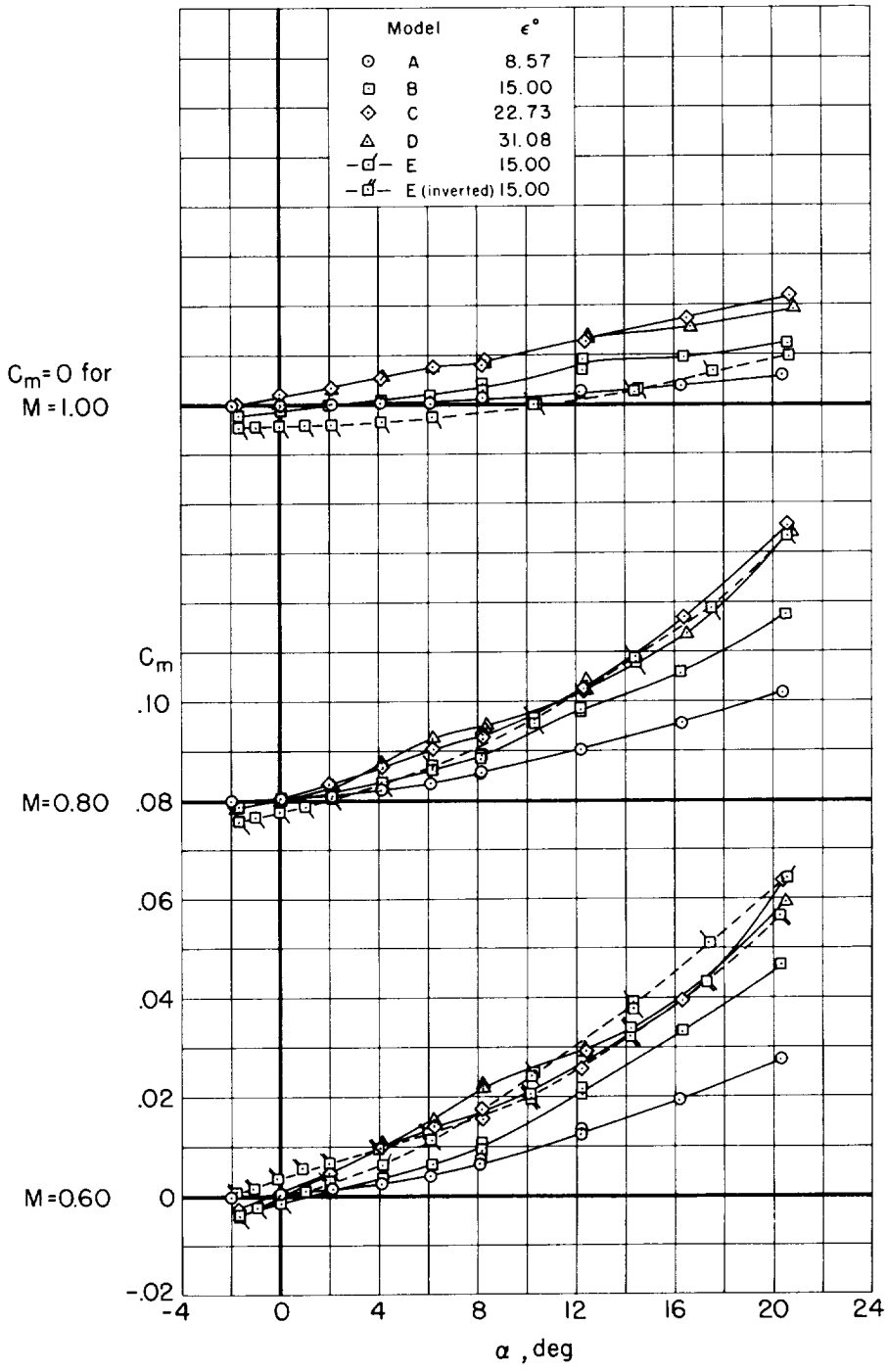

(a) M = 0.60, 0.80, and 1.00

Figure 4.- Variation of forebody pitching-moment coefficient with angle of attack.

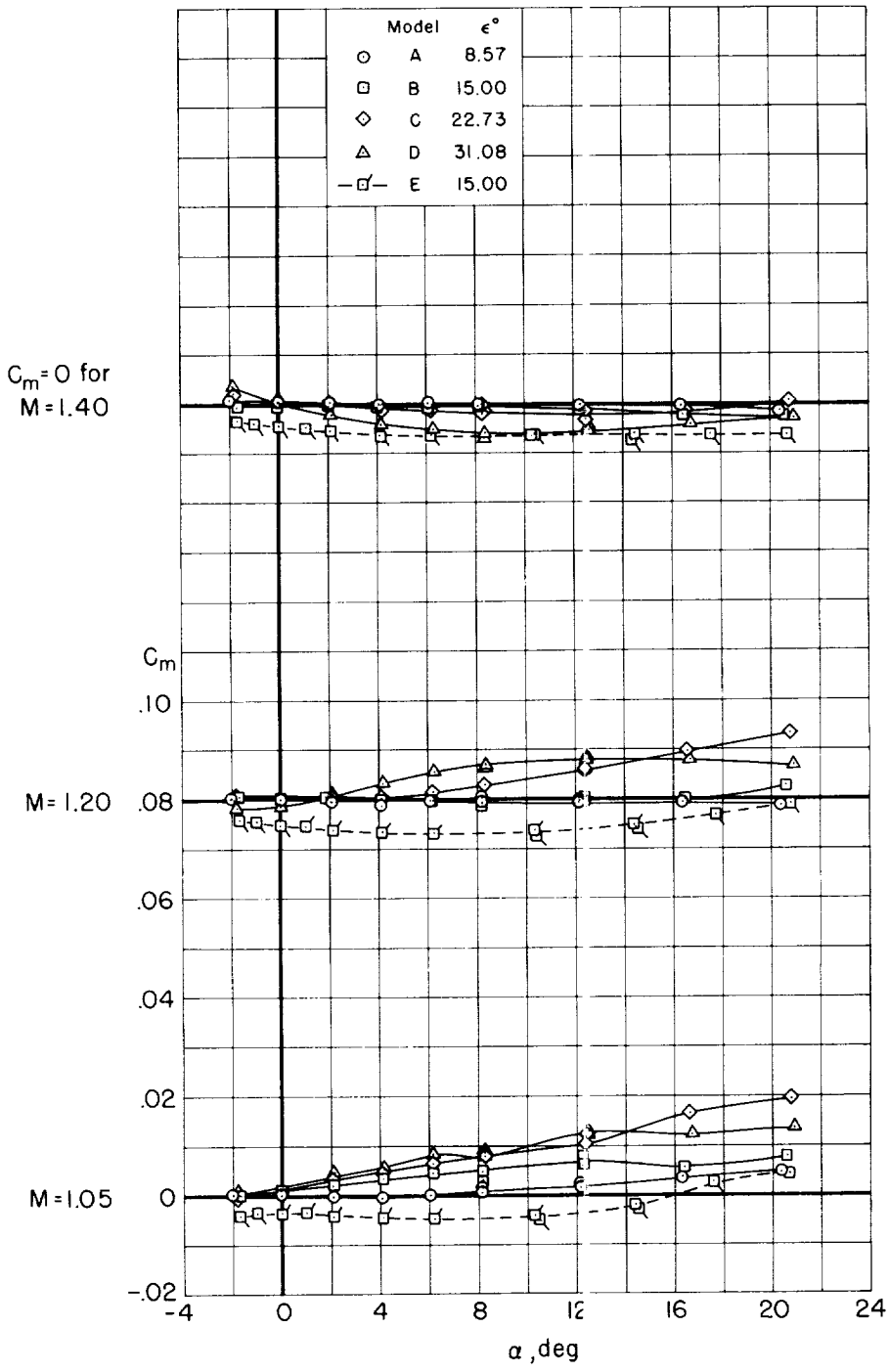

(b) M = 1.05, 1.20, and 1.40

Figure 4.- Concluded.

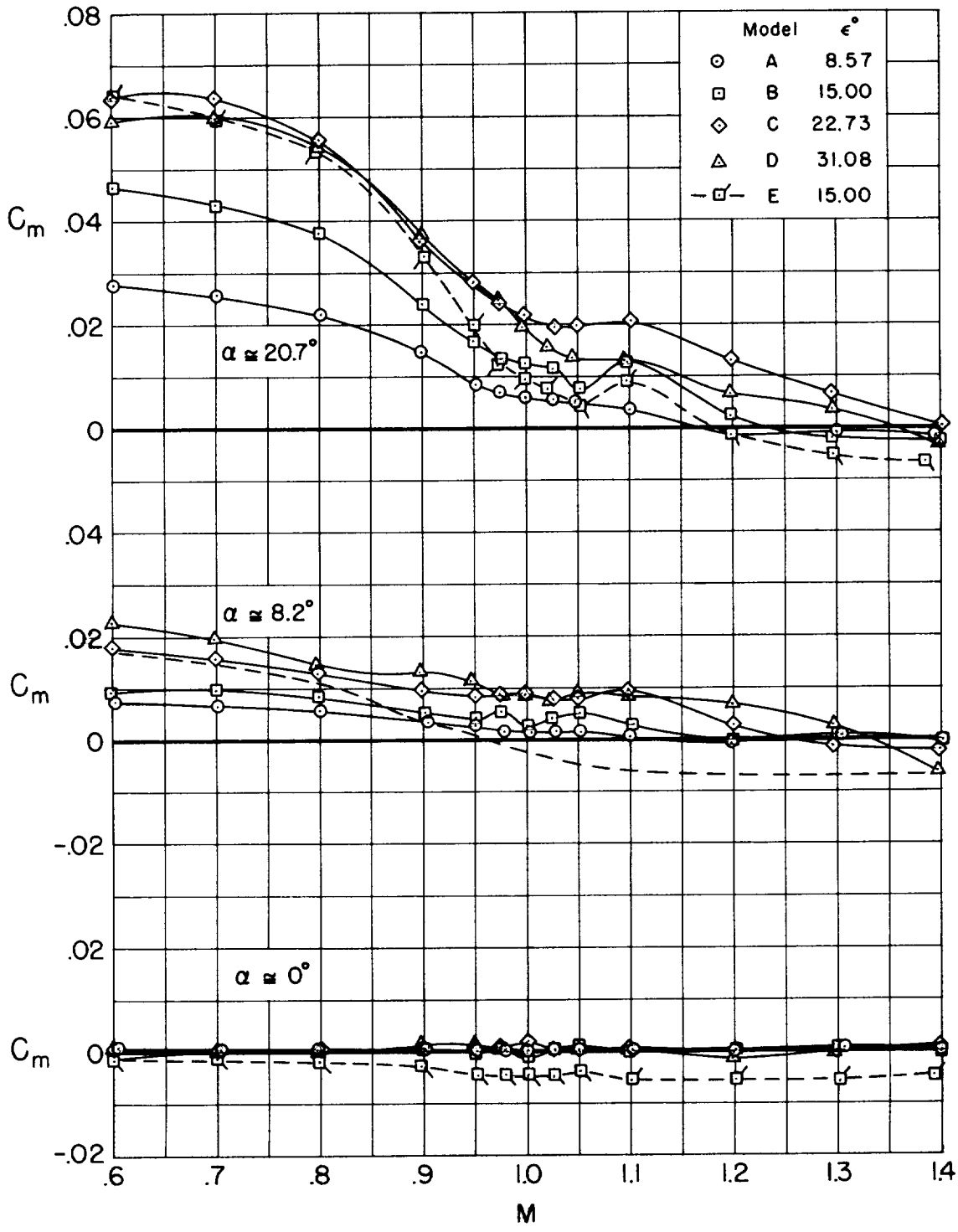

Figure 5.- Effect of Mach number on forebody pitching-moment coefficient.

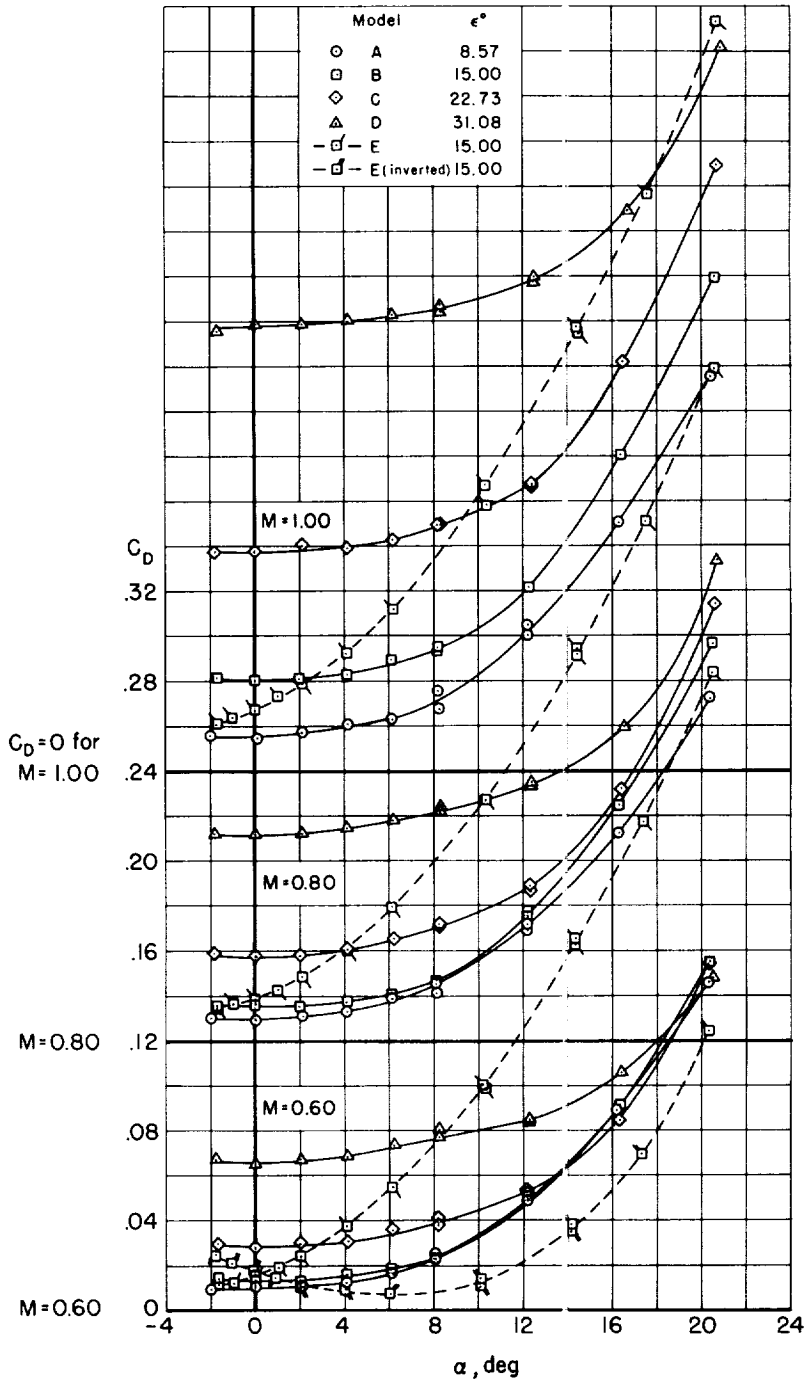

(a) M = 0.60, 0.80, and 1.00

Figure 6.- Variation of forebody drag coefficient with angle of attack.

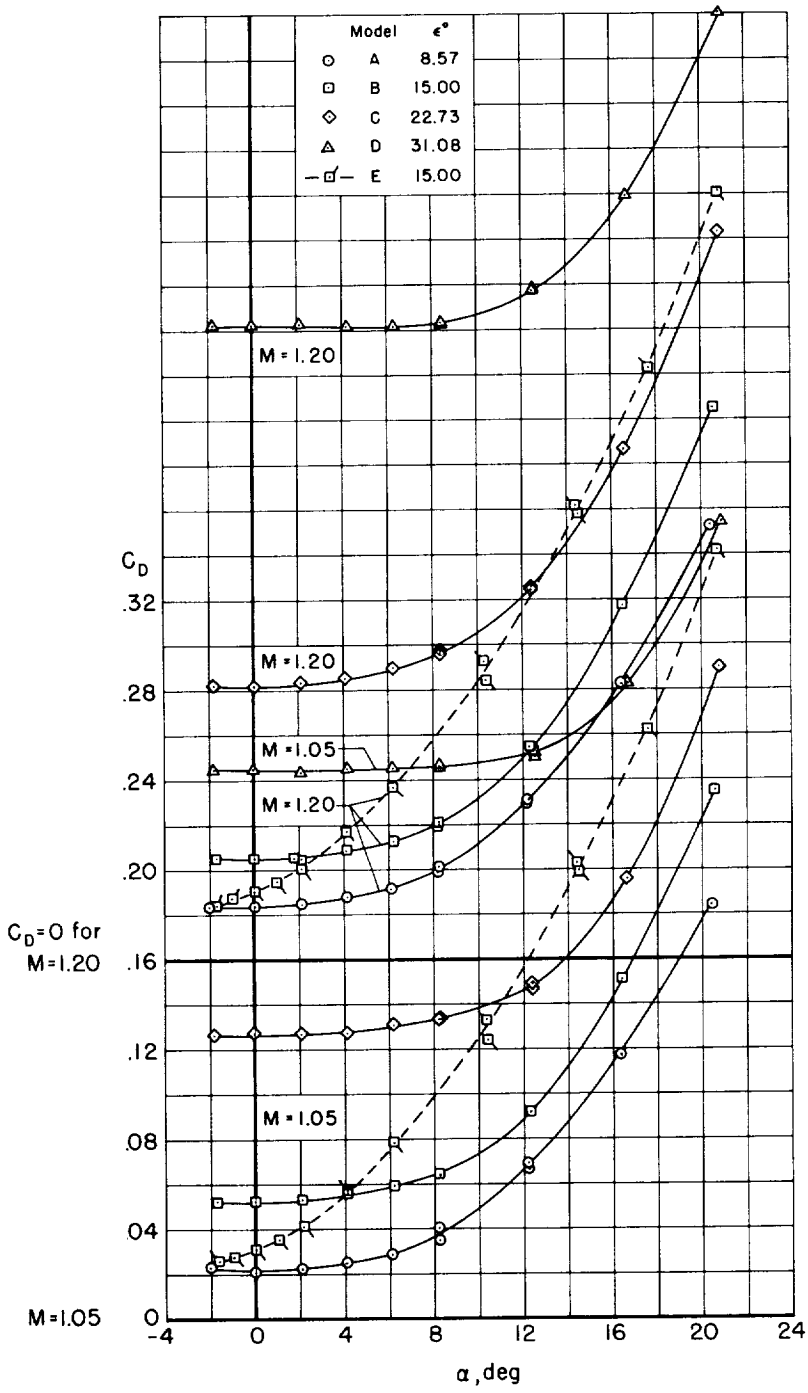

(b) M = 1.05 and 1.20

Figure 6.- Continued.

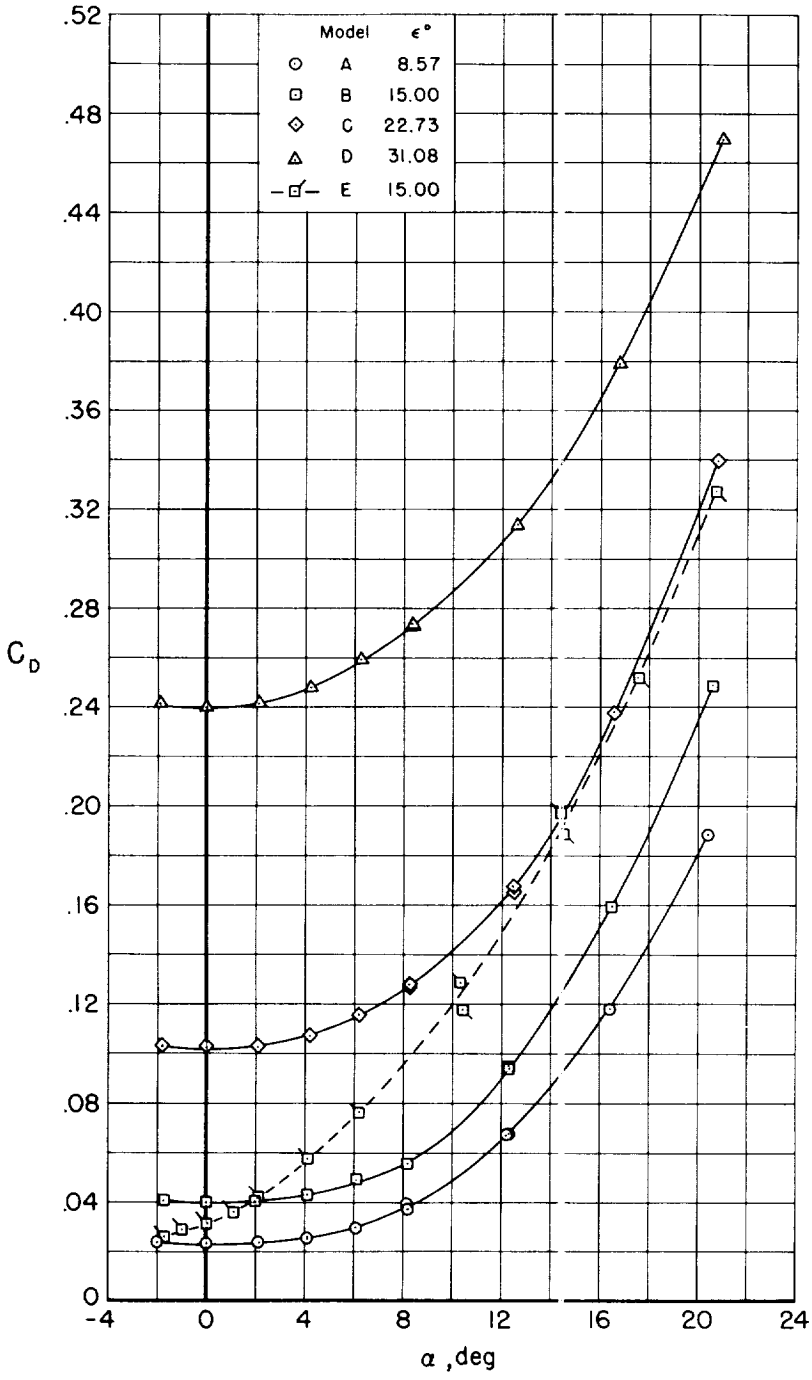

(c) M = 1.40

Figure 6.- Concluded.

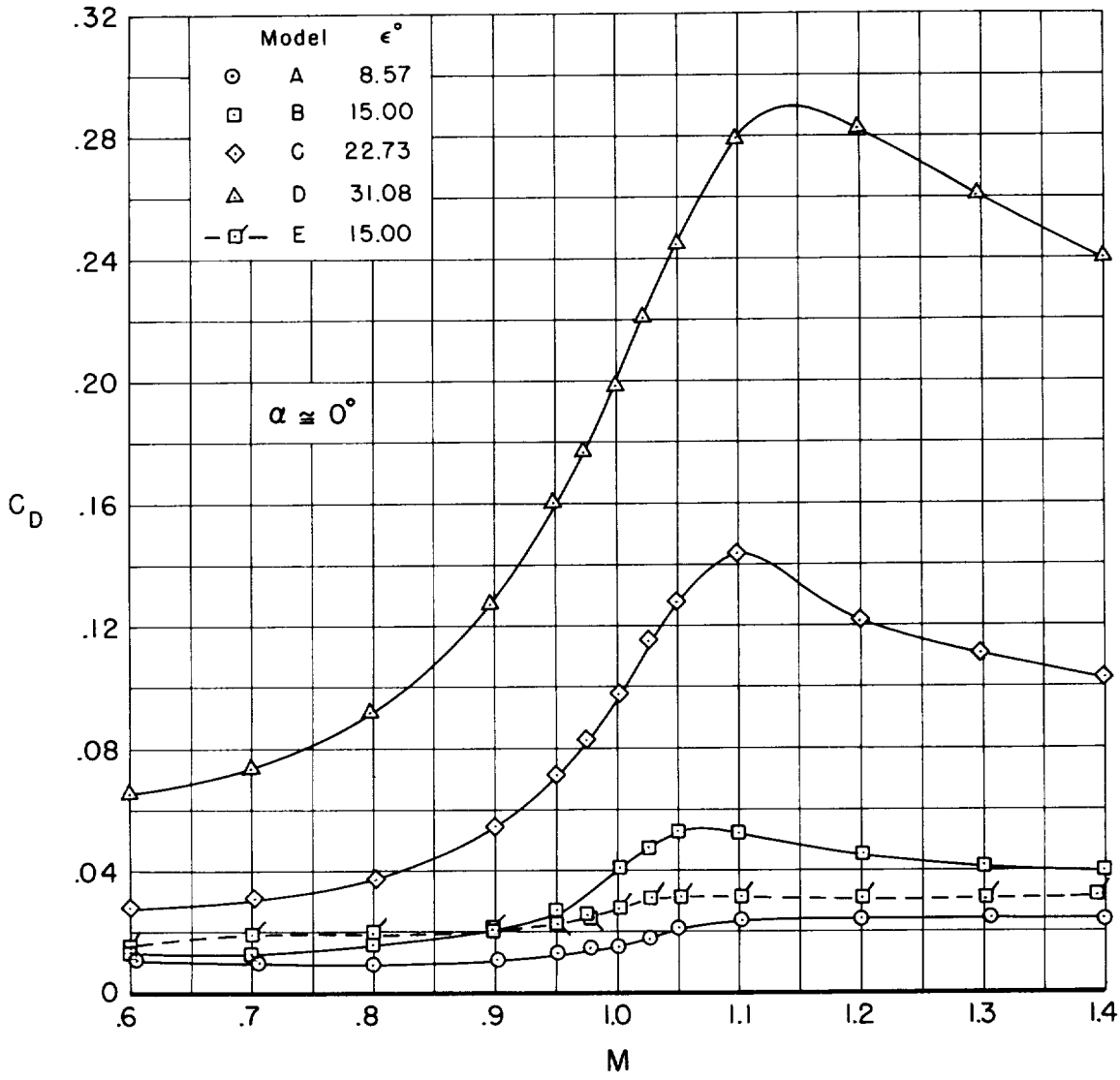

(a) $\alpha \cong 0°$

Figure 7.- Effect of Mach number on forebody drag coefficient.

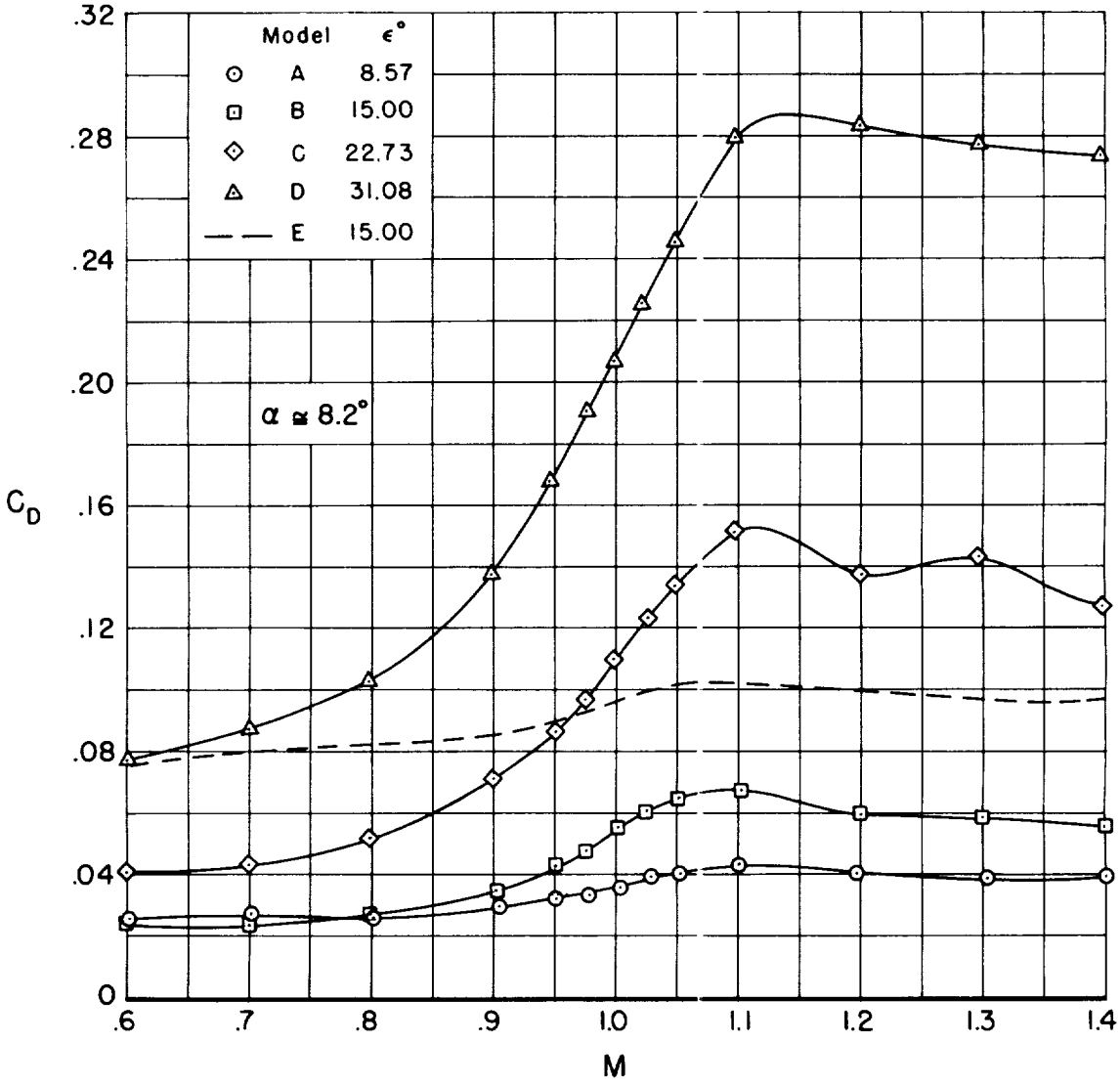

(b) $\alpha \cong 8.2°$

Figure 7.- Continued.

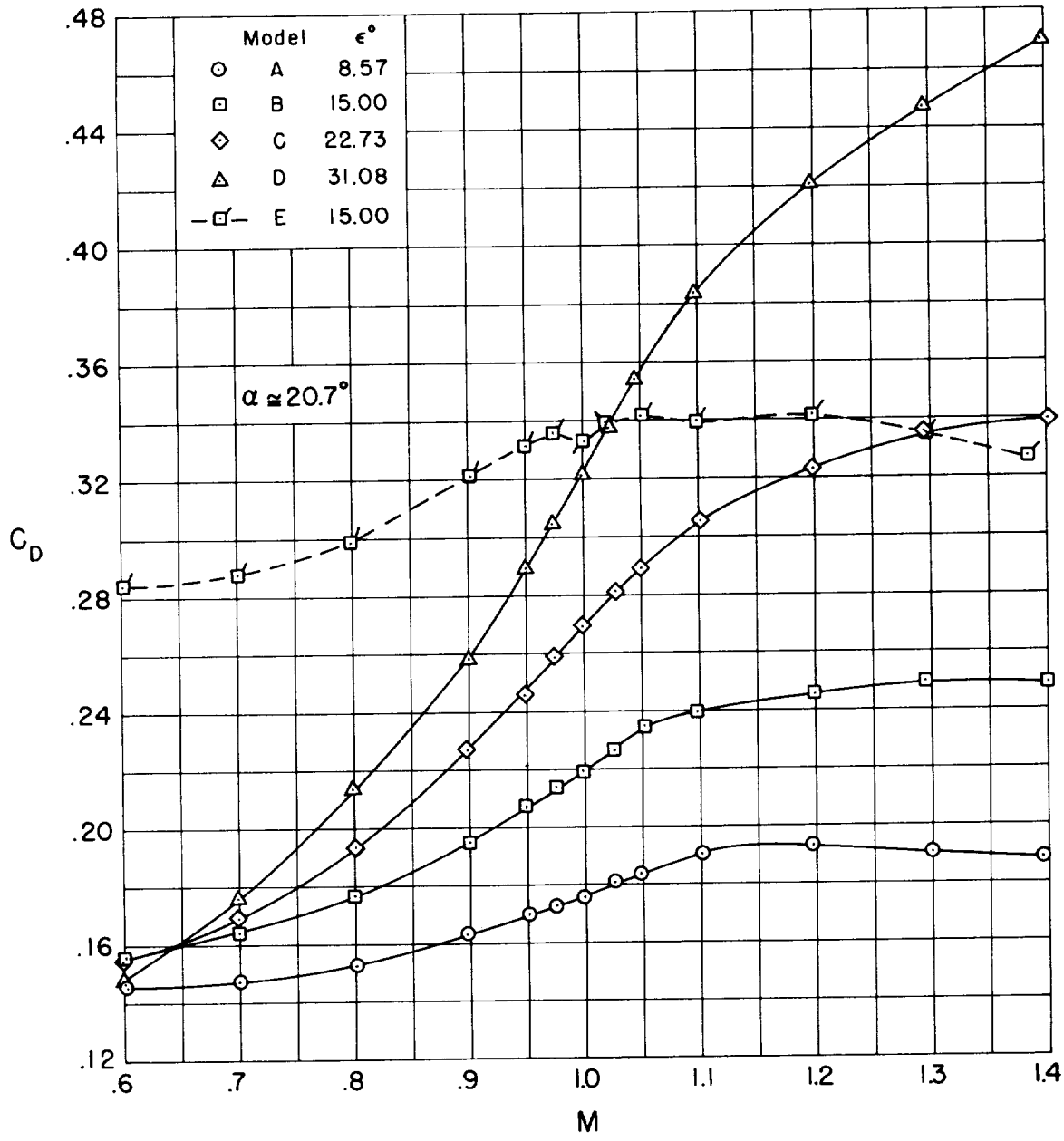

(c) $\alpha \cong 20.7°$

Figure 7.- Concluded.

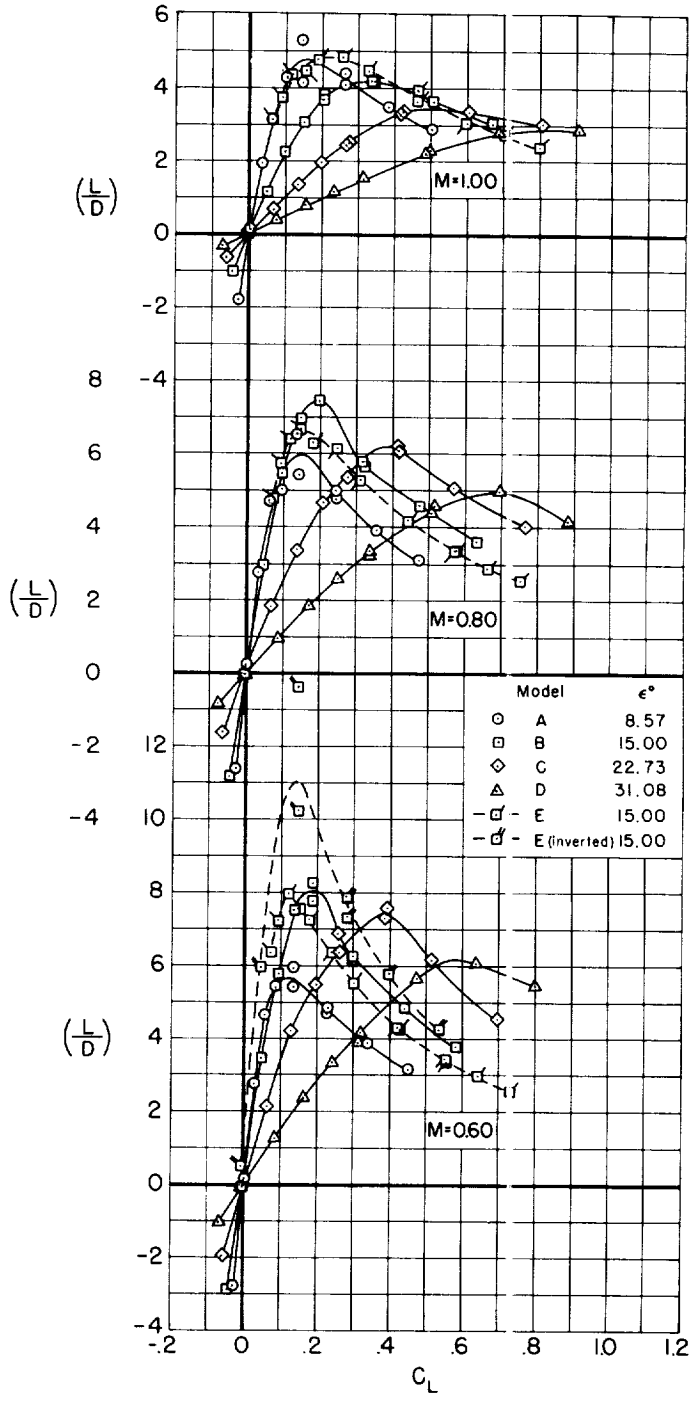

(a) M = 0.60, 0.80, and 1.00

Figure 8.- Variation of forebody lift-drag ratio with lift coefficient.

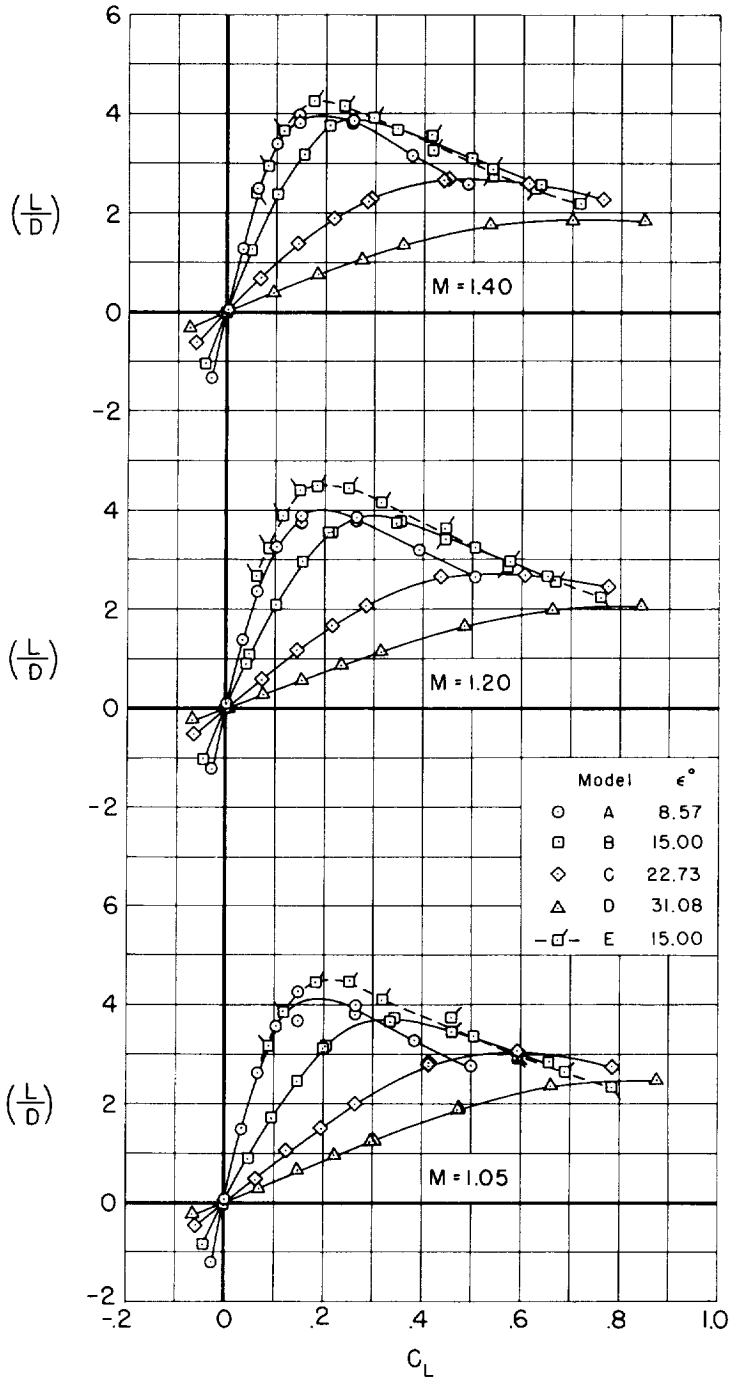

(b) M = 1.05, 1.20, and 1.40

Figure 8.- Concluded.

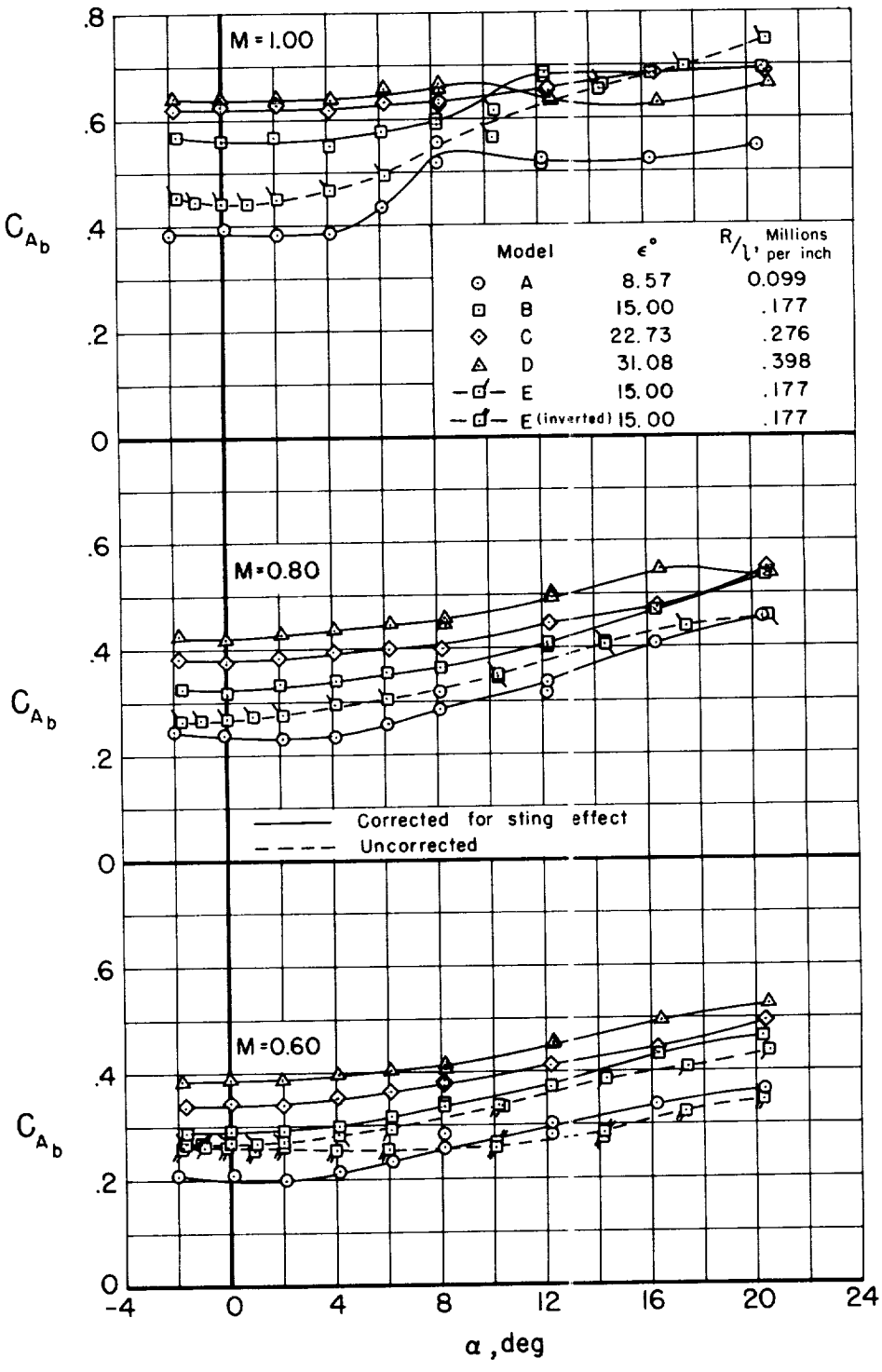

(a) M = 0.60, 0.80, and 1.00

Figure 9.- Variation of base axial-force coefficient with angle of attack.

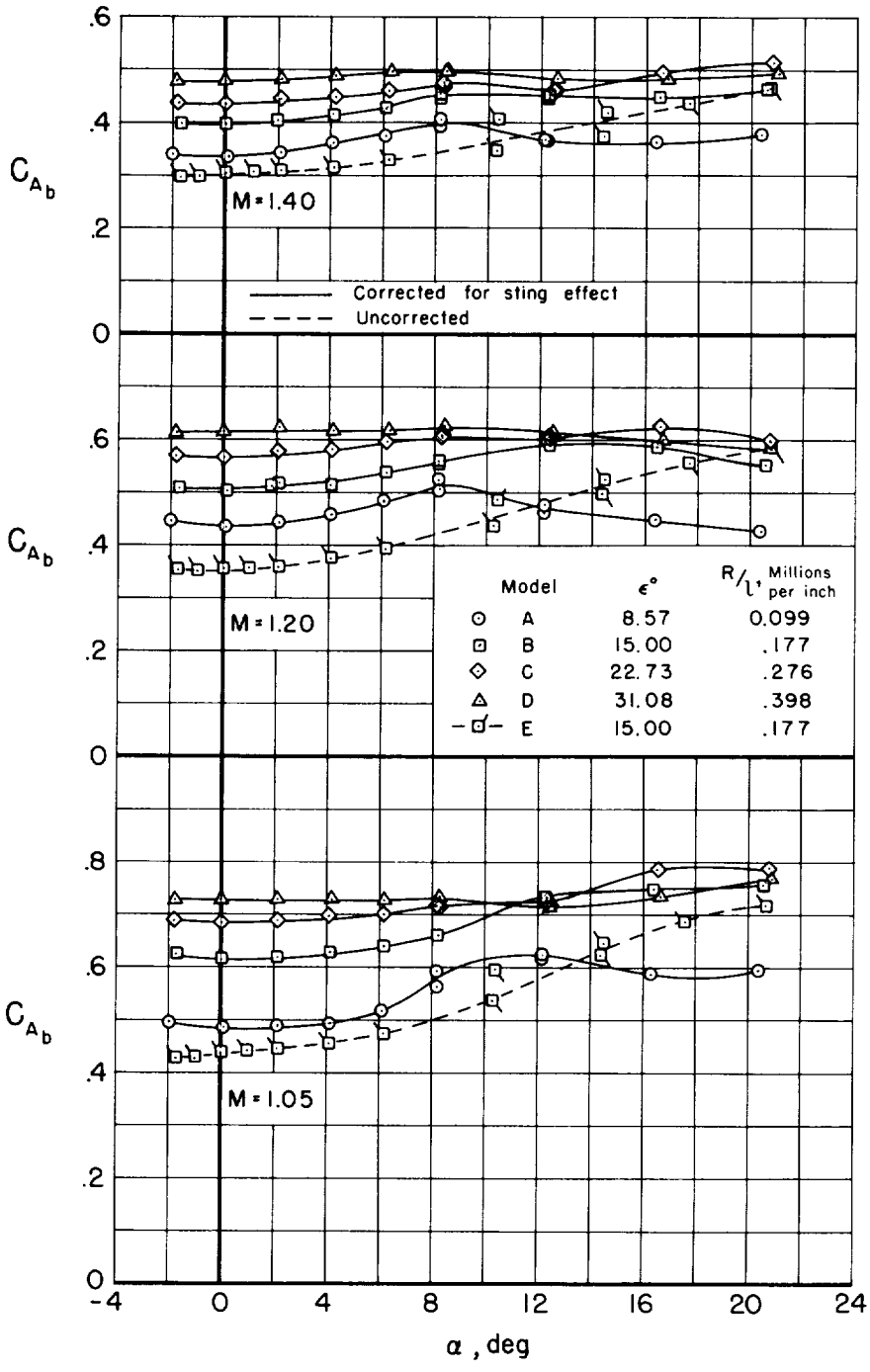

(b) M = 1.05, 1.20, and 1.40

Figure 9.- Concluded.

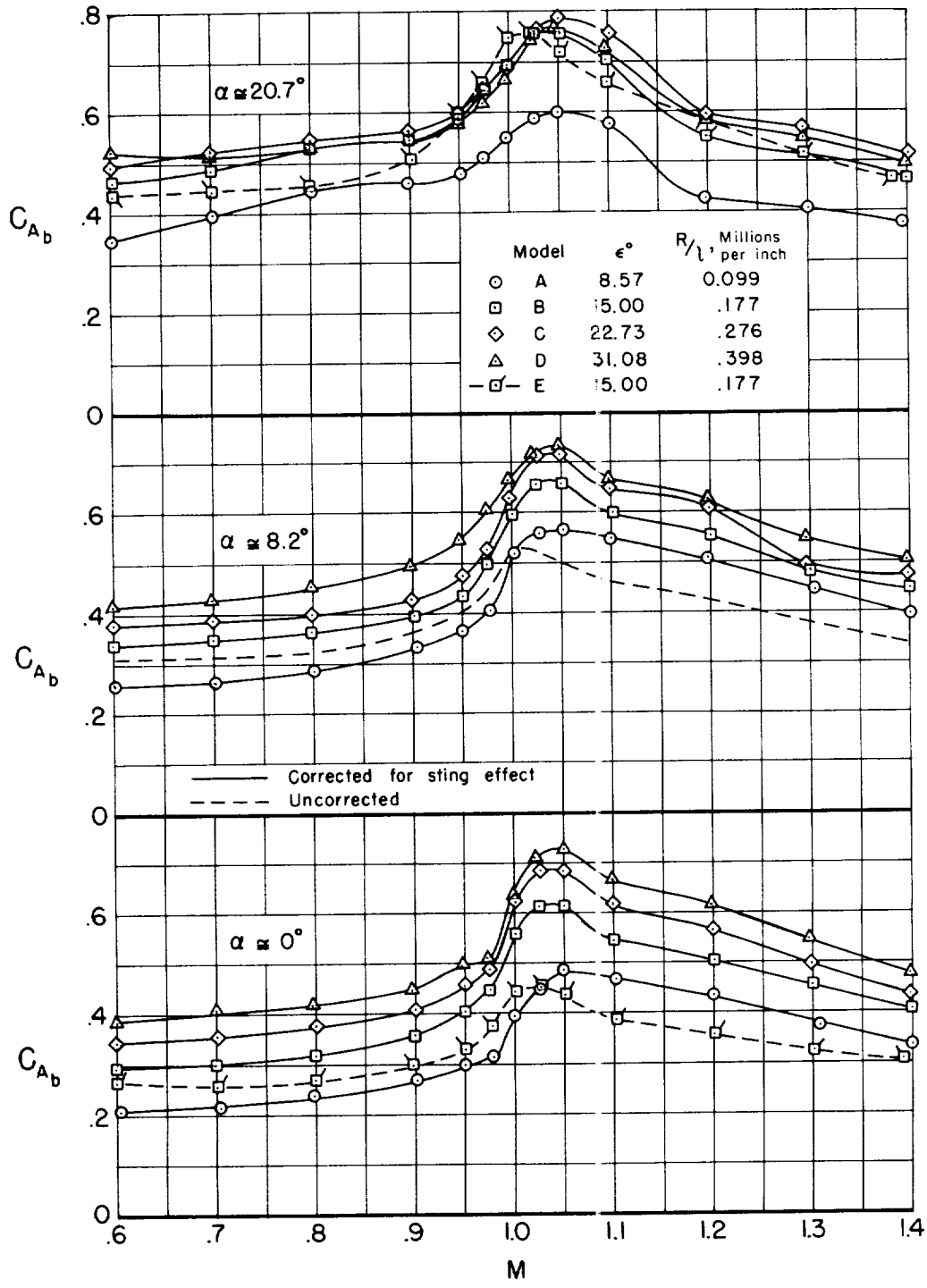

Figure 10.- Effect of Mach number on base axial-force coefficient.

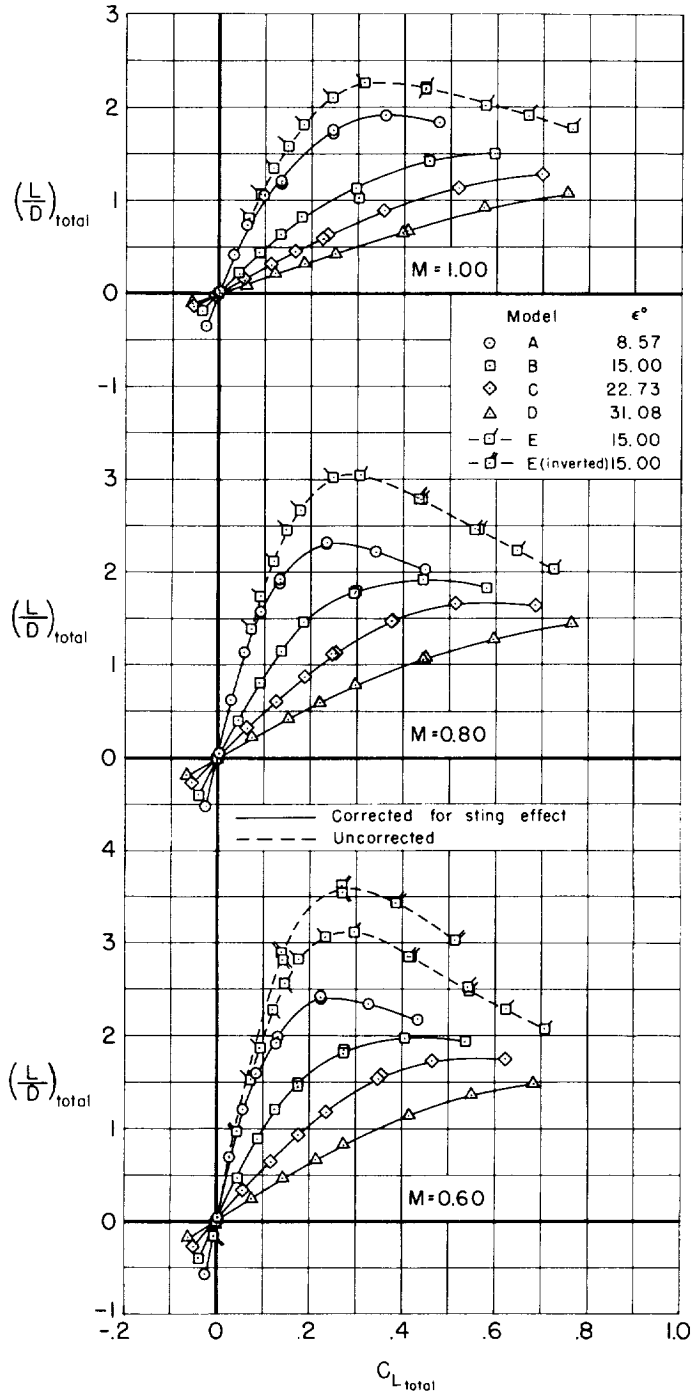

(a) M = 0.60, 0.80, and 1.00

Figure 11.- Lift-drag ratios for the forebody and base combined.

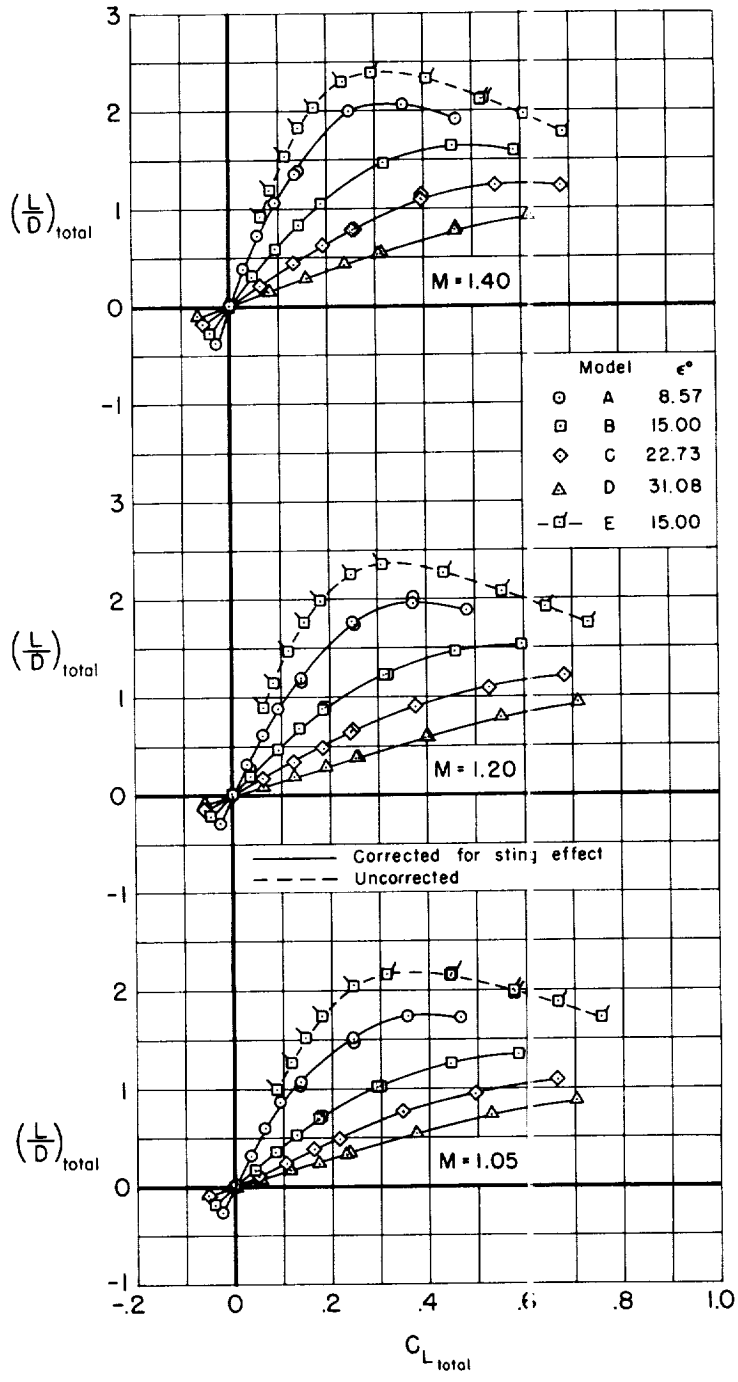

(b) M = 1.05, 1.20, and 1.40

Figure 11.- Concluded.

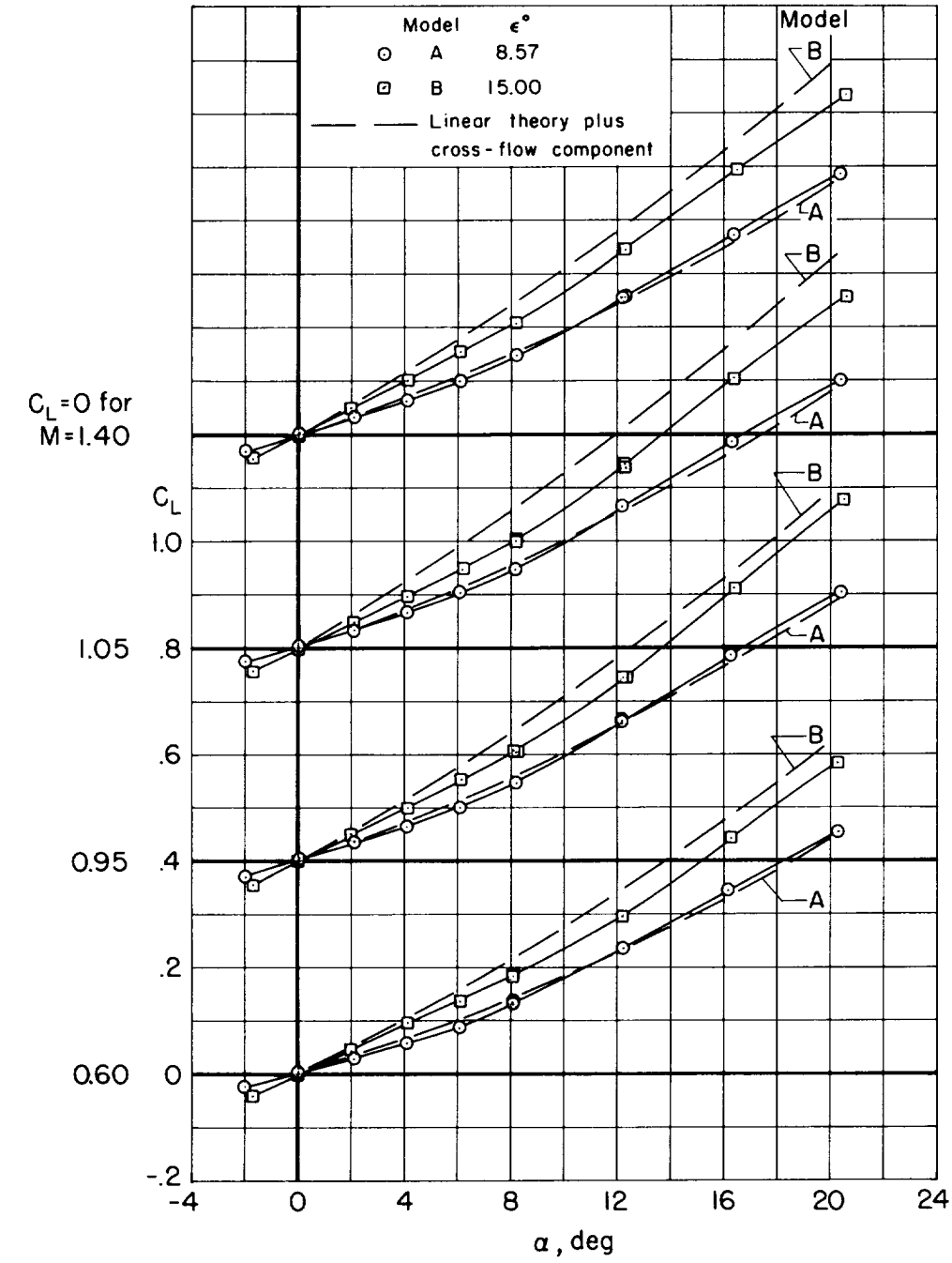

(a) Models A and B.

Figure 12.- Comparison of calculated and experimental lift curves for the elliptic cones.

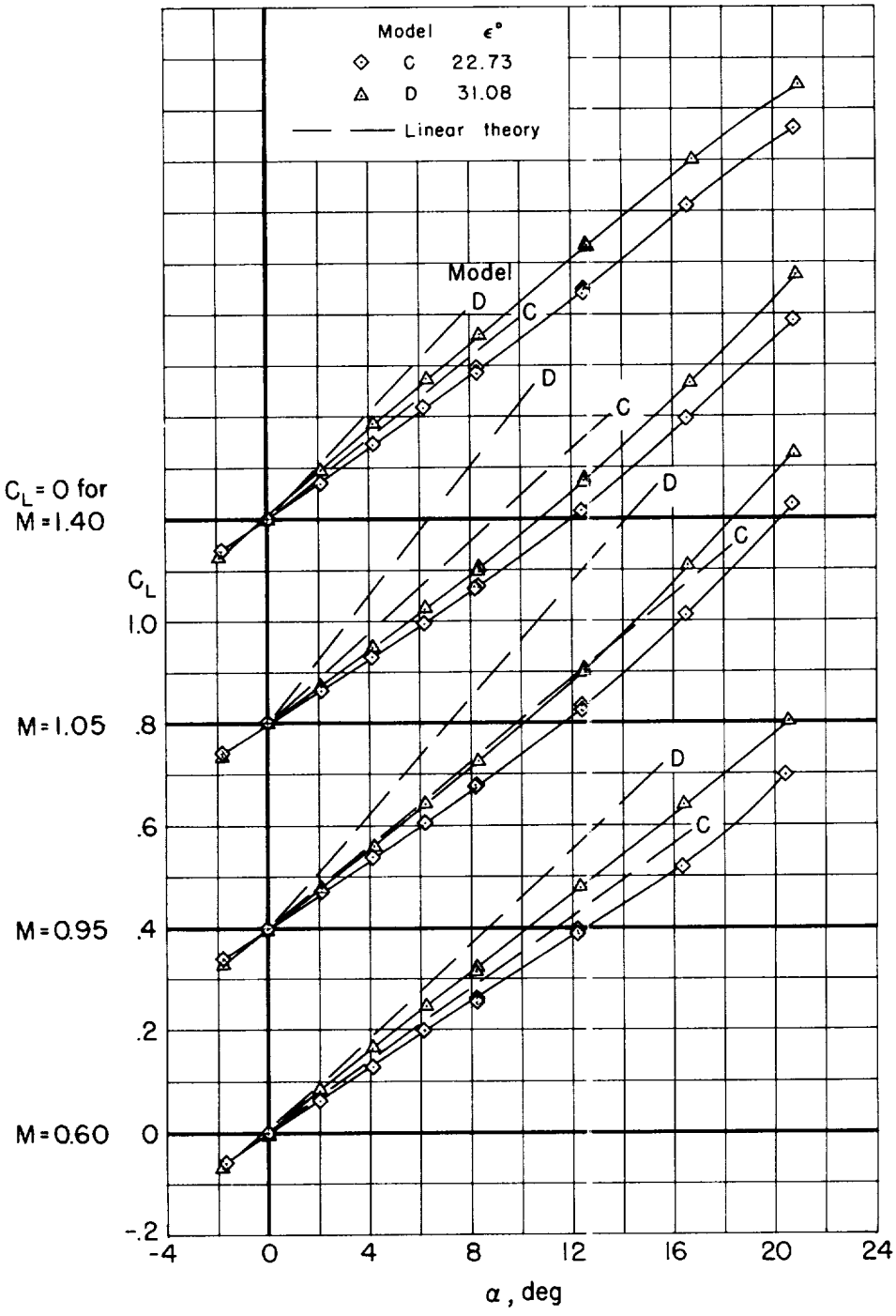

(b) Models C and D.

Figure 12.- Concluded.

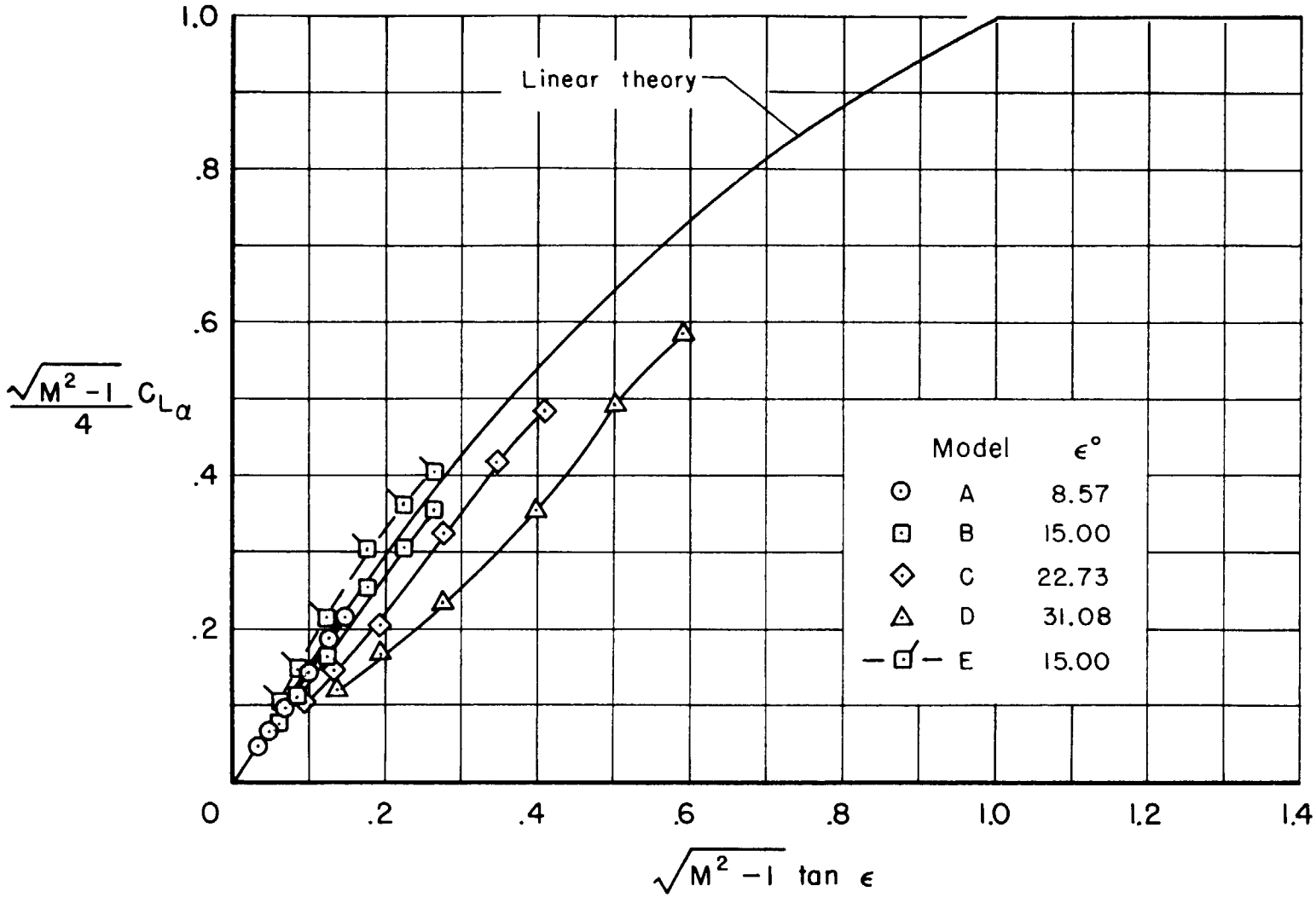

Figure 13.- Comparison of experimental lift-curve slopes with those given by linear theory, M > 1.

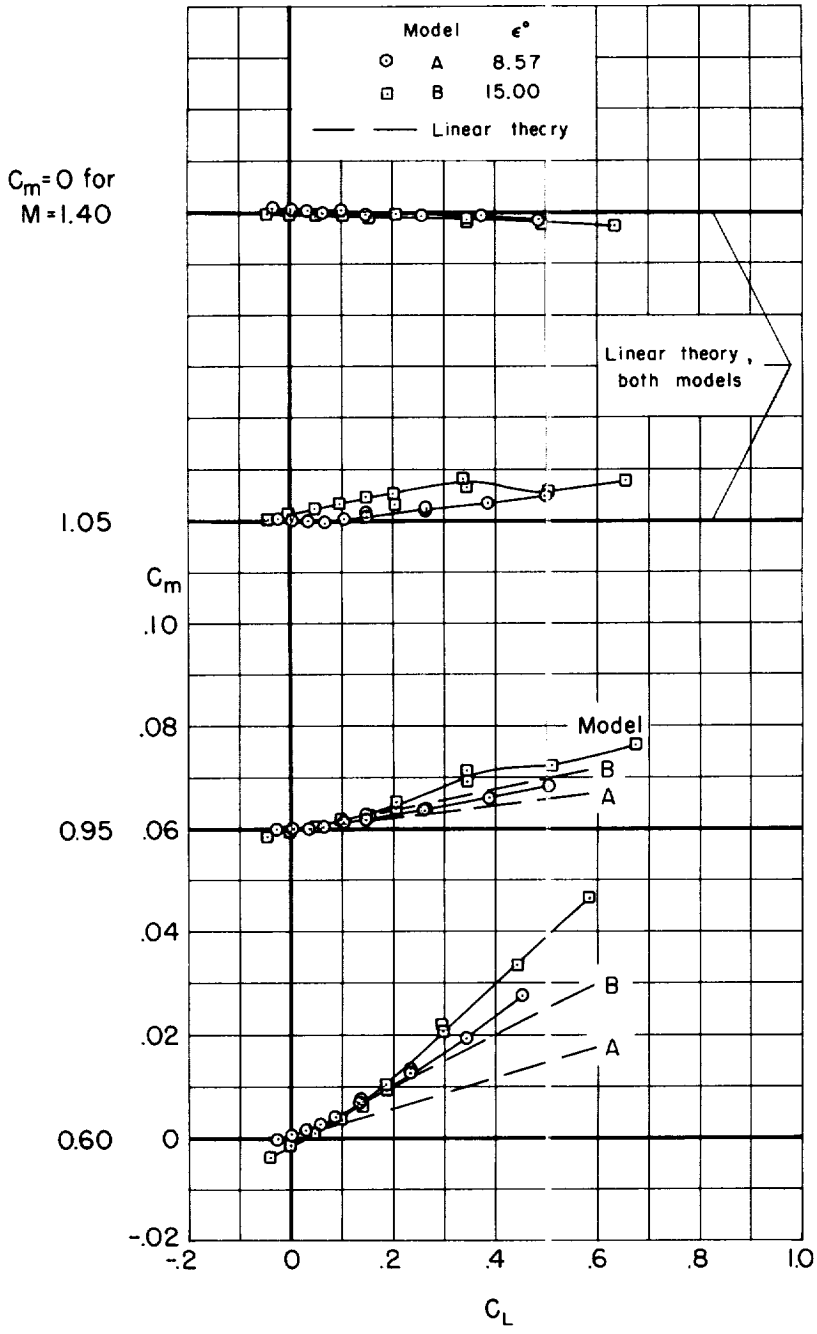

(a) Models A and B.

Figure 14.- Comparison of calculated and experimental pitching-moment curves for the elliptic cones.

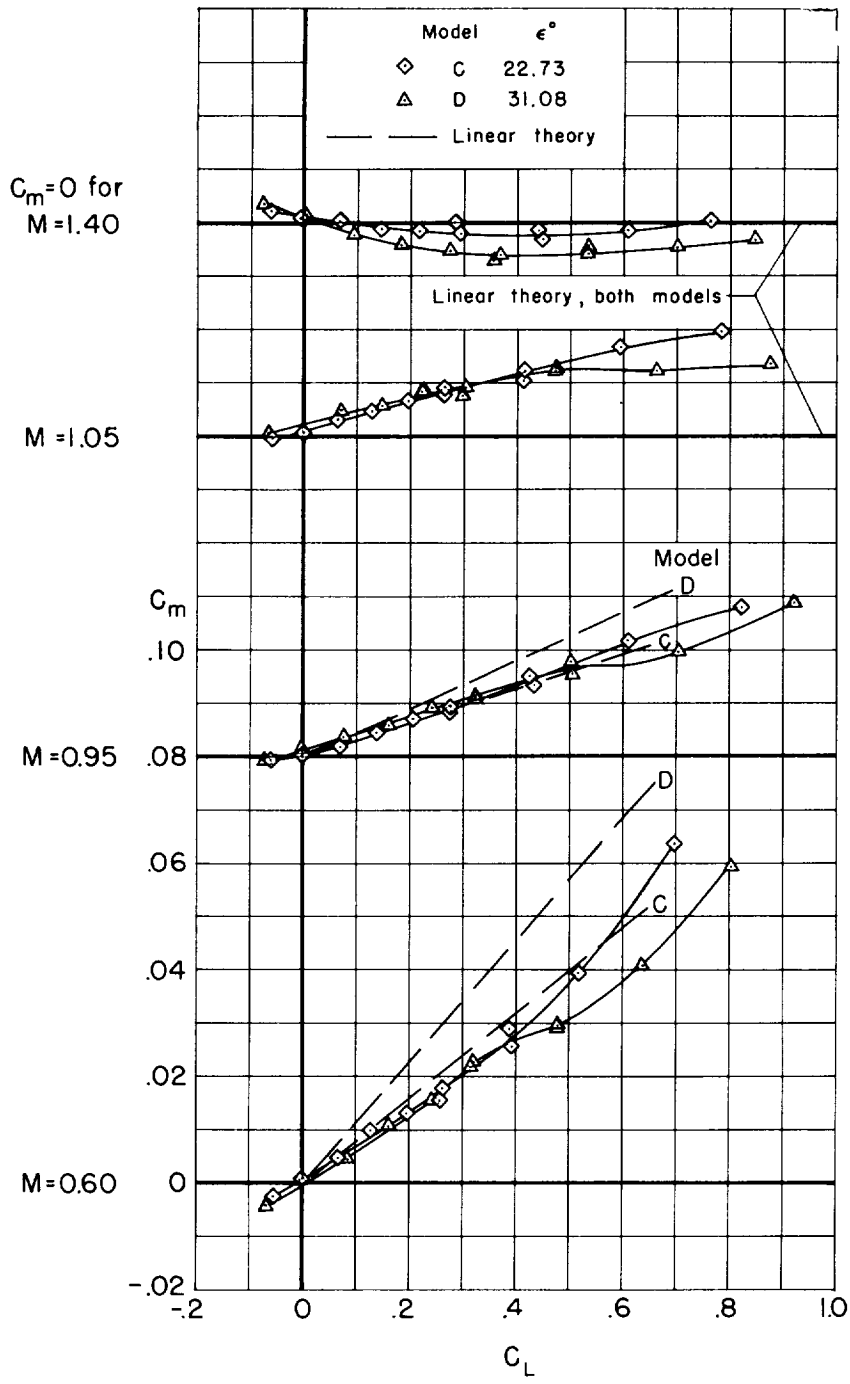

(b) Models C and D.

Figure 14.- Concluded.

NASA-Langley, 1961 A-548